ELIoT

Enhance Lighting for the Internet of Things

DELIVERABLE: D5.3

public summary report with non-sensitive information from WP5

Contract number:	825651
Project acronym:	ELIoT
Project title:	Enhance Lighting for the Internet of Things
Project duration:	1 January 2019 – 30 June 2022
Coordinator:	Volker Jungnickel, Fraunhofer Heinrich Hertz Institute, Berlin, Germany

Deliverable Number:	D5.3
Type:	Report
Dissemination level:	Public
Date submitted:	30.06.2022

Authors:	MXL
Partners contributed	FHG, UOXF, TU/e, MXL, SIG

This project has received funding from the European Union's Horizon 2020 research and innovation programme under grant agreement No 825651 (ELIOT)

Abstract

Deliverable D5.3 describes different mechanisms for power reduction in Internet of Things (IoT) devices that use Light Communications (LC) as studied in the EU horizon 2020 ELIOT project. The document is a public summary of the findings within the WP5 of the project.

In this report, various aspects of power reduction are examined. In particular, communication link budget improvements and baseband processing. Most results are by now publicly available in open literature and a reference to these results is provided in the text.

The report also gives an outlook on how the result can be valorised in products and standards, especially in the ITU G.hn series of Recommendations.

This project has received funding from the European Union's Horizon 2020 research and innovation programme under grant agreement No 825651 (ELIOT)

1 Executive summary

This report describes research directions in reducing power consumption of Light Communication (LC)-enabled IoT systems. In a system, the consumed power can be classified into communication link budget aspects (that is the power consumed by analogue transmitter/receiver frontends) and baseband processing power. In a concluding chapter this report discusses how these can influence the use of available silicon by making modifications to firmware and how it can enhance standards, in particular ITU G.hn series of Recommendations.

The following research directions are assessed:

Communication Link Budget:

- Tx Efficiency
  - Improvement of the light-emitting source and its driver circuits can help to reduce the transmitter's power consumption while delivering the required optical transmitted power. We argue that impedance matching, as it is popular in RF, may not lead to the most efficient driver design.
  - Suitable operation of the LED
- Rx Sensitivity
  - Design of a high-sensitivity Rx can help reduce the required received optical power, and hence the transmission power. A prime technology studied is the photonic concentrator.

Baseband Processing:

The way that an LED responds to an input signal differs from an RF antenna. The bandwidth is subject to LED junction properties: it is low-pass but it also blocks very low frequencies near DC. Despite the low-pass nature, there is only a gentle decline above the 3 dB bandwidth. The consumed power to generate non-negative signals is subject to LED properties and highly non-linear. The electrical consumed power is not necessarily proportional to the signal variance.

Different modulation schemes have different requirements for the power consumption of the LED driver and the required signal processing complexity, leading to different demands for power consumption. Besides, there is an inevitable trade-off between spectrum efficiency and energy efficiency which requires investigations into appropriate modulation schemes for IoT.

We compared ACO, FLIP and DCO OFDM. These have been studied extensively before, but ELIOT added a number of relevant insights:

- we argue that on-off keying or PAM can be an attractive alternative to OFDM. For links with a very strong signal with respect to the noise floor DCO-OFDM appeared to outperform PAM, particularly because OFDM can more easily be adapted to exploit frequencies far above the LED bandwidth. For PAM, thus would require a large amount of pre-emphasis, or equalization at the receiver. The noise enhancements can be large, but a suitably chosen (adaptive) rate, a

This project has received funding from the European Union's Horizon 2020 research and innovation programme under grant agreement No 825651 (ELIOT)

careful choice between, in particular 2-PAM (OOK) and 4-PAM and a decision feedback equalizer can make PAM competitive also substantially above the 3 dB bandwidth. However, we noticed a limited appetite in literature to study time-domain equalizers. These can be complex to study, particularly if the number of taps needs to large. However, to compensate for short comings of optical-to-electrical conversion, we showed that limited complexity can suffice.

- ACO-OFDM and Flip OFDM have been proposed to avoid the use of a DC bias. It was known that ACO and Flip OFDM schemes, in their basic form, do not use 50% of the signal space available, thus lack spectrum efficiency. As new insights, we proved that the typical FFT-based receivers combine signals in a way that leads to a 3 dB penalty in signal-to-noise ratio, which was not explained in earlier papers. The non-negative clipping spreads 50% over the signal energy of the entire band, which is not recuperated during FFT based signal recovery. We believe that these new ELIOT insights can explain why ACO and Flip OFDM in practical tests did not seem to have a distinct attractiveness over DCO-OFDM.
- Spectrum and power efficiency: In a few ELIOT papers, we challenge and refine commonly made statements about the spectrum efficiency of OFDM versus PAM and show that both load the same number of signal dimensions, i.e., spectrum efficiency is equal but the way that dispersion is address differs. We observed that several earlier works do not clearly distinguish between the emission bandwidth of the LED, the widening of this optical spectrum due to intensity modulation, and the bandwidth available in the electrical-to-electrical channel. We challenge a commonly made statement that optical OFDM loses 50% of efficiency due to a required Hermitian symmetry.
- For OFDM, we propose as way to exchange SNR values to better exploit the discrete nature of QAM constellations. ITU G.9991-type of power loading of OFDM loses 1.5 to 3 dB by using QAM constellations with an integer number of bits. We propose as way to recuperate this loss, using a number of additions and subtractions across adjacent subcarriers.
- It can be attractive to invert the non-linear distortion which occurs due to the LED, as it can reduce power consumption by 70%.
-

The choice of the LED and its operation point

Although illumination LEDs are chosen for a large quantum efficiency, for communications also a large 3 dB bandwidth is preferred. A trade-off is postulated empirically, in the form of a rule of thumb: “transmit power raised to the power alpha times bandwidth raised to the power one minus alpha” appears to be an LED constant. We found a theoretical justification for such a model, where current density acts as a parameter to make the trade-off.

According to communication theory, the achievable bit rate grows approximately linearly with an increasing bandwidth but approximately logarithmically with the received energy per bit. However, this needs to be reviewed for a gentle low-pass roll-off of the LED response, as it allows modulation far beyond the 3 dB bandwidth. These lead to a perspective on how to operate the LED: a system design faces the challenge to trade-off power versus bandwidth according to the physics LED

This project has received funding from the European Union’s Horizon 2020 research and innovation programme under grant agreement No 825651 (ELIOT)

properties, to optimize a communication throughput target. We investigated how bandwidth and efficiency depend on LED choices and what would be appropriate choices.

This project has received funding from the European Union's Horizon 2020 research and innovation programme under grant agreement No 825651 (ELIOT)

2 Contents and Lists

2.1 Acronyms

AP	Access Point
AWGN	Additive White Gaussian Noise
BAT	Bit Allocation Table
CP	Cyclic Prefixes
EQE	External Quantum Efficiency
FEC	Forward Error Correction
IEEE	Institute of Electrical and Electronics Engineers
ITU	International Telecommunications Union
LC	LiFi Controller
LiFi	Light Fidelity
LOS	Line of sight
MAC	Medium Access Control
MIMO	Multiple Inputs – Multiple Outputs
NPB	Normalized Power Budget
OFDM	Orthogonal Frequency-Division Multiplexing
OFE	Optical Front End
OOK	On-Off Keying in the
PAM	Pulse Amplitude Modulation
PAPR	Peak-to-Average Power Ratio
PHY	Physical Layer
PLC	Powerline Communications
PM	Pulsed Modulation
POF	Plastic Optical Fiber
PSD	Power Spectrum Density
QoS	Quality of Service
RF	Radio Frequency
SISO	Single Input-Single Output
SNDR	Signal to Noise and Distortion Ratio
SNR	Signal to Noise Ratio
TIA	Trans Impedance Amplifier
VLC	Visible Light Communication
WPE	Wall Plug Efficiency
ZF	Zero Forcing

This project has received funding from the European Union's Horizon 2020 research and innovation programme under grant agreement No 825651 (ELIOT)

2.2 List of Figures

This project has received funding from the European Union's Horizon 2020 research and innovation programme under grant agreement No 825651 (ELIOT)

2.3 List of Tables

This project has received funding from the European Union's Horizon 2020 research and innovation programme under grant agreement No 825651 (ELIOT)

2.4 Tables of contents

This project has received funding from the European Union’s Horizon 2020 research and innovation programme under grant agreement No 825651 (ELIOT)

This project has received funding from the European Union's Horizon 2020 research and innovation programme under grant agreement No 825651 (ELIOT)

3 Introduction

The number of Internet of Things (IoT) devices has been growing at a steady pace over the past decade, at an average annual growth rate of 15% in the next half decade. Meanwhile, the growth of the number of mobile phones still grows although as the market penetration may already be near saturation. Within the ELIOT project, we further foresee an important class of devices for which the required bit rates and quality of service (QoS) are highly demanding. That is, bit rates are not only large because collectively many devices generate large amounts of traffic, but also individual devices, for instance in an industry setting, exchange large amounts of data. For this reason, a wide range of power consumption regimes, e.g., varying from a door lock to a drone in a factory capturing high resolution low latency uncompressed video, are relevant and need to coexist in the architecture foreseen in ELIOT. The power consumed by an IoT device for wireless communication highly depends on:

i) **frontend power** This is determined by both the transmitter (Tx) efficiency and receiver (Rx) sensitivity. Cell layout (e.g., to support distributed Multi Input Multi Output (MIMO) links) and interference management also have a significant impact on frontend power.

ii) **baseband signal processing power.** A baseband processor mainly implements a PHY layer for modulation and demodulation and higher layer protocols. An appropriate choice of the modulation scheme is determined by the medium access control (MAC) layer controlling the PHY layer. The PHY layer indicates feasible modulation schemes, depending on received signal and interference plus noise, and the MAC chooses either robust or optimum options. In addition, the MAC layer assigns the transmission opportunities to the connected device. Baseband processing power can be substantially reduced by switching off devices when they are not being used.

iii) The choice of **modulation method:** Modulation methods have been compared for OWC in numerous papers. In the ELIOT project, we revisited these by theoretical analyses and found insight that refine popular statements in literature. An overview in Chapter 5 gives a summary. Different modulation schemes have different requirements for the power consumption of the LED driver and the required signal processing complexity, leading to different demands for power consumption. Besides, there is an inevitable trade-off between spectrum efficiency and energy efficiency which requires investigations into appropriate modulation schemes for IoT. In particular,

- We argue that on-off keying or Pulse Amplitude Modulation (PAM) can be an attractive alternative to Orthogonal Frequency Division Multiplexing (OFDM). For links with a very strong signal with respect to the noise floor, DC Offset DCO-OFDM appeared to outperform PAM, particularly because OFDM can more easily be adapted to exploit frequencies far above the LED bandwidth. For PAM, thus would require a large amount of pre-emphasis, or equalization at the receiver. The noise enhancements can be large, but a suitably chosen (adaptive) rate, a careful choice between, in particular 2-PAM (OOK) and 4-PAM and a decision feedback equalizer can make PAM competitive also substantially above the 3 dB bandwidth. However, we noticed a limited appetite in literature to study time-

This project has received funding from the European Union's Horizon 2020 research and innovation programme under grant agreement No 825651 (ELIOT)

domain equalizers. These can be complex to study, particularly if the number of taps needs to large. However, to compensate for short comings of optical-to-electrical conversion, we showed that limited complexity can suffice. See also Chapter 6

- We study strategies to load power over the modulation spectrum in Chapter 7.
- We study the spread of power over multiple LEDs in a MIMO scheme in Chapter 12.
- We compare ACO, FLIP and DCO OFDM: ACO-OFDM and Flip OFDM have been proposed to avoid the use of a DC bias. In DCO-OFDM, this bias corresponds to three or four times the rms value of the modulation, but the use of ACO comes with a severe penalty. We address this in Chapter 13. Firstly, these schemes, in their basic form, do not use 50% of the signal space available. Secondly, the typical FFT-based receivers combine signals in a way that gives a 3 dB penalty in signal-to-noise ratio. More precisely, the non-negative clipping spreads 50% over the signal energy of the entire band, which is not recuperated during FFT based signal recovery. This at the same time, this refined the claim that OFDM is attractive because every symbol is only subject to the response of one channel at one frequency. In fact, only 50% of the symbol energy is subject to the response of the specific subcarrier, the remain 50% of that symbol energy is subject to all other frequency responses, the FFT detector discards this portion of the symbol energy. We believe that these insights can explain by ACO and Flip OFDM in practical tests did not seem to have a distinct attractiveness over DCO-OFDM.
- For OFDM, we propose a way to exchange SNR values to better exploit the discrete nature of QAM constellations (Chapter 14.4): To avoid overhead and to repair a loss caused by the use of OFDM QAM constellations with an integer number of bits, we exploit the mostly monotonously declining frequency response of the concatenation of an LED, a slightly dispersive propagation channel and a photodiode and TIA response. We propose improvement to recover a 1.5 dB loss due to discrete constellations and avoid excessive overhead in negotiating bit loading profiles. (Chapter 14)
- LED second-order distortion: A concern with the use of OFDM that we identified [1], [2] [3] [4] is the distortion by the LED (chapter 9). We argue that repairing the non-linearity by dedicated signal processing can save 50% of transmit power, particularly at high bit rates, and large constellation, say when a gigabit or more is to be carried by typical LEDs of 3 dB bandwidth of a few tens of MHz [5]. (Chapter 11)
- Spectrum and power efficiency: In a few ELIOT papers, we challenge and refine commonly made statements about the spectrum efficiency of OFDM versus PAM

    - Number of dimensions: We can model the electrical channel between LED current and the received current coming out of a photodiode as a low-pass real channel. The number of signal dimensions available in an interval T is 2TBw, regardless of whether PAM or OFDM is used.

This project has received funding from the European Union’s Horizon 2020 research and innovation programme under grant agreement No 825651 (ELIOT)

- Factor one half penalty for spectrum efficiency of IM-DD: Thus, while OFDM is not spectrally more efficient [6] [7] [8], and while Hermetian symmetry to force a purely real signal is not causing a ½ penalty in achievable throughput if we consider the capacity of an electrical low-pass channel, as we debated in [7], one may identify a ½ penalty from the use IM-DD if we compare the optical spectrum efficiency if the emitter were a perfectly monochromatic source [6]. However, for proper color rendering, visible light LED emit a spectrum that is 1000 times the width of the entire radio spectrum. If we modulate a couple of hundreds of megabit/s, that is done at an optical spectrum efficiency of about one millibit/s/Hz. Evidently in IR, narrower emitters can be used, but optical spectrum efficiency is not a serious constraint, as LC allows very dense (atto-cell) spatial reuse of the spectrum. Yet, the spectrum but also the power efficiency in the electrical and intensity modulation path are key concerns in the choice of modulation method.

iv) The choice of the LED, its current density and the optical system. See Chapter 8.

- While illumination LEDs are chosen for a large quantum efficiency, for communications also a large 3 dB bandwidth is preferred. In the LED, electron hole pairs recombine radiatively (thereby emitting a photon) or non-radiatively (causing a leakage current and reducing EQE). Non-radiative recombination also contributes to the response speed of the LED and increases its 3 dB bandwidth. On the other hand, a reduction in effective optical power may counterproductively lead to an inadequate signal-to-noise ratio. A trade-off is postulated empirically, in the form of a rule of thumb: "transmit power raised to the power alpha times bandwidth raised to the power one minus alpha" appears to be an LED constant. This semi-empirical model gives straight lines on a log-log scale. ELIoT searched for a theoretical justification for such a model, where current density acts as a parameter to make the trade-off .
- According to communication theory, the achievable bit rate grows approximately linearly with an increasing bandwidth but approximately logarithmically with the received energy per bit. However, this needs to be reviewed for a gentle low-pass roll-off of the LED response, as it allows modulation far beyond the 3 dB bandwidth. These lead to a perspective on how to operate the LED: a system design faces the challenge to trade-off power versus bandwidth according to the physics LED properties, to optimize a communication throughput target.
- Narrowing down the width of the optical beam emitted from the LED is a very effective way to save power. This topic was out of scope of this WP.

This project has received funding from the European Union's Horizon 2020 research and innovation programme under grant agreement No 825651 (ELIOT)

A list of potential improvement opportunities was identified during the early phases of ELIOT project and the most promising ones where further investigated. Table X provides an overview of the project´s findings.

Table 1: Possible power-saving technologies.

Possible technologies	Gains	Difficulty
Series transistor-based VLC transmitter	Moderate	High
Switching modulator	Moderate	Low but limited to OOK/ PAM
Fluorescent concentrator	Moderate	Medium
Retroreflector	High for very low data rate	High
LED choice and current density	Moderate	Low
MIMO (cell) layout, optics	Moderate	High
Pulsed modulation	Significant	Medium
Bit loading	Moderate	Medium
Unipolar OFDM	Significant	Low
Sleep mode	Significant	Low
Half duplex operation	Significant	Low
Discontinuous operation	Significant	Low
Alternative modulation for low-power IoT	Substantial	
SNR exchange between subcarriers (MC-CDMA)	1.5 to 3 dB	Medium
Non-linearity Compensation	70% less power or 50% more throughput	Medium / High
Narrow beams	large	large

This project has received funding from the European Union's Horizon 2020 research and innovation programme under grant agreement No 825651 (ELIOT)

4 IoT Devices and Their Power Consumption

Power can be reduced by measures that increase the efficiency of emitting light, as in section 4.1, or by increasing the sensitivity of the receiver, as in Section 4.2. Yet in many cases, only the (battery) power in the client is critical. An extreme solution is to make the client device passive, i.e., without actively radiating, as in Section 4.4.

4.1 Transmitter optimization for low power

4.1.1 Possible TX Technologies

Linear VLC modulators are mainly classified into direct switched mode power supply (SMPS), Bias-T and series transistor topologies. Directly steering from a SMPS can only be used for low bandwidth applications. The Bias-T topology can be used but it may require inductor and decoupling capacitor sizes that would not allow extensive miniaturization. In applications where OFDM signals above 2 MHz are considered, the inductor and capacitor sizes do not need to be that large. However, for PAM of OOK, the blocking of near DC frequencies can be problematic and demands line coding (see section 6.2.3)

A series transistor-based topology is suitable for a wide range of modulation frequencies, with compactness and compatibility with most of the modulation methods such pulse amplitude modulation (PAM) and orthogonal frequency-division multiplexing (OFDM). It drives the LED as a current source, thus from a high impedance source.

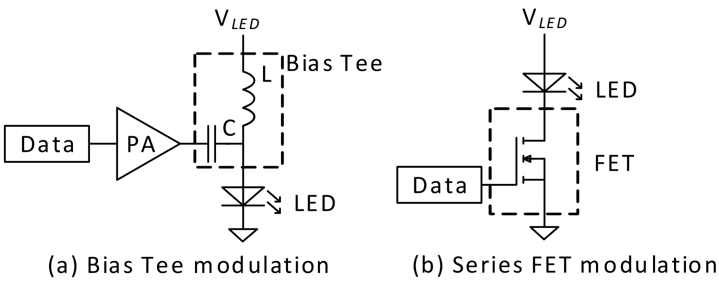

Figure 1: Two main approaches to linear modulator topologies

Bias-T based transmitter: Unlike radio frequency modulation, which can be bipolar, LED intensity modulation is unipolar. A common laboratory practice for VLC modulation is to apply a DC offset such that the waveform can be transmitted by light. The Bias-T circuit has the advantage that the amplifier separately supplies the AC current for modulation while the DC bias is delivered from the power supply and decoupled by the Bias-T. A typical power amplifier (PA) used from radio RF engineering, has 50 Ohm impedance, while the LED has only few Ohms of impedance. We can already observe that for DC-free baseband transmission (say 2 .. 100 MHz) via a low-ohmic LED, the choice of the bias T components and the PA output impedance are very critical and may require bulky components.

In particular, the DC blocking may remove an essential signal spectrum at low frequencies that can lead to baseline wander, and cause problems with prolonged sequences or all zeros or all ones.

This project has received funding from the European Union's Horizon 2020 research and innovation programme under grant agreement No 825651 (ELIOT)

Series Transistor for LED modulation: In this topology, a transistor is placed in series with the LED to control its current. A field-effect transistor (FET) is suitable for high current applications, i.e., the modulation of LEDs. Low manufacturing costs and reduced switching losses distinguish FETs, making it the most used transistor type worldwide for analogue and digital circuits [11]. Similar to BJTs, FETs have a complex output impedance and are therefore well suited for LED driving. The circuit symbol and a basic FET modulation circuit are depicted in Figure 1. The voltage-controlled FET is biased with a constant voltage applied to the gate.

Among the many differences between the bias-T and the series transistor is the output impedance of the driver towards the LED, which is very small and very large, in the respective topologies. The next section addresses the question how this affects the efficiency, as either solution seemingly violates principles of impedance matching.

4.1.2 Impedance matching for LED

LEDs have a dynamic resistance of a fraction of one Ohm. This is substantially lower than the 50 Ω impedance for which amplifiers and most lab bias-T modules are typically built. Nonetheless we see that LEDs are directly connected to a bias-T, via 50 Ω cabling. In the setup mismatched at 50 Ω output to a low LED impedance, which is used in most academic papers, the LED time constant is large and bandwidth is low. However, if the driver does impedance matching, driver + LED bandwidth can be significantly higher, assuming the same parasitic capacitance of the LED. The main mechanism can be seen as impedance matching, not pre-emphasis.

The Maximum Power Theorem states that maximum power is transferred from source to load if the load resistance R_L equals the source resistance R_S. We argue that the converse of this principle may not be used to find the most efficient modulator design.

The converse (best choice for output impedance is to equal the load impedance) is not necessarily valid and “optimized for highest power” does not equals “optimized for highest efficiency”.

Our conclusion, elaborated in ELIOT work, is that insights from optimizing the power extraction for an RF amplifier may not simply be reused without careful reconsideration. We also note that circuit design for very low impedances and a wide relative band (DC to 200 MHz) is a skill in itself.

4.1.3 Switching modulator for pulse modulation

The previous sections described linear drivers. Besides losses in (mis) matching, both topologies have more losses: the bias-T has losses because it needs a class B amplifier. The series transistor has losses because it acts as a Class A amplifier and the transistor needs to conduct the DC current as well. These losses were elaborated in [9, 10]. In section 6.2, Fraunhofer HHI explains that PAM can effectively be used for good throughput and can allow very power-efficient switching modulators.

There are also system-level methods to reduce the amount of power needed

- Sectorization and optimization of the light emission pattern via free form optics. Signify presented results in [11].

This project has received funding from the European Union’s Horizon 2020 research and innovation programme under grant agreement No 825651 (ELIOT)

- Optimization of the choice of the LED and its current density. Signify and TU/e presented results at [12]. See also chapter 8, entitled “Optimized current density of the LED ”
- Making the receiver more sensitive. We present results in Section 4.4.

4.2 Efficiency in the electrical-to-optical-to-electrical channel

In the LED, we distinguish the light extraction efficiency, the forward voltage efficiency to reflect that, according to the Shockley equation, the LED voltage is higher than the photon energy strictly requires, the internal quantum efficiency (IQE) and a thermal droop. The IQE depends on the number of carriers in the Quantum well QW.

We further refer from our “Sectorization” paper at SPIE Photonics West 2022[[12] and to the introductory section of several earlier papers. The efficiency by which the LED converts electrical power into a photon flow that contributes to the communication link can be decomposed in various factors.

4.3 Power efficiency of Electrical driving

The transmit electrical power P_T is a function of the mean and variance of the current. We argued that in contrast to what is claimed in several paper outside ELIoT, the average transmit power is not the average of the current square. In the junction voltage is fairly constant, such that the average power into the LED can well be approximated as the junction voltage times the average current.

We conclude that the assumption in many papers that the electrical power consumed in the transmitter equals the $second$ monent is an oversimplification and that further refinements of the transmitter design can possibly improve the power efficiency. This has for instance led to the consideration of Class D modulators for OOK.

4.4 Retro-reflecting link topologies

4.4.1 Overview

One direction of investigation within Eliot has been the development of a low power tag for IOT applications. Figure 7 shows a schematic of the low power tag and base station. The base station provides both illumination and communications to and from the tag. The downlink (from base station to tag) operates by modulating the illumination source, and a receiver on the tag is used to detect and decode this.

The uplink, from tag to base station, uses a novel retro-reflecting link. Figure 8 shows the tag. A retroreflective sheet, which is commonly used on road signage, directs light from the base station that is incident on the tag back to the base station, where an optical receiver is situated. A liquid crystal shutter which can vary its contrast when a voltage is applied, is then placed in front of the retroreflector to modulate the returning light which can then be detected at the base station.

This project has received funding from the European Union’s Horizon 2020 research and innovation programme under grant agreement No 825651 (ELIOT)

Such a system requires considerably less power than an LED based transmitter, as the tag has no source of light. This allows the tag to operate at very low power.

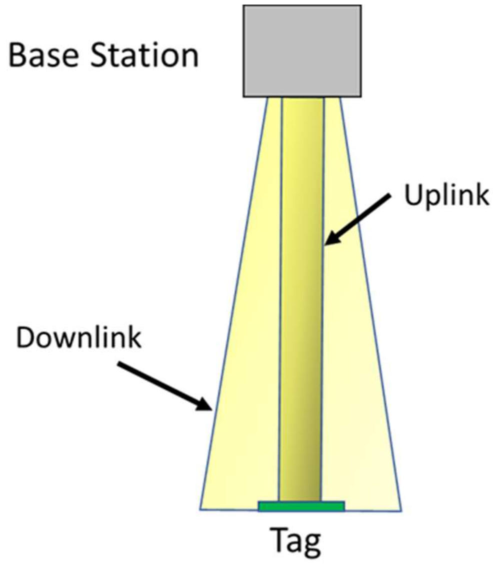

Figure 2: Schematic of Tag-Base station system.

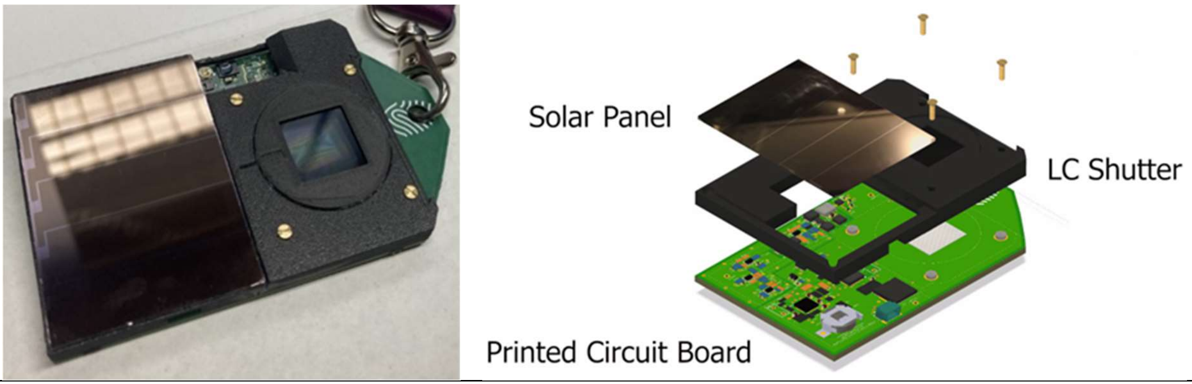

Figure 3: Picture of completed tag with exploded view.

The tag also has a solar panel to provide self-sufficient operation without the need for charging. The tag uses a low power ambident light sensor which can trigger the controller on board to shutdown along with the receiver circuitry for the downlink if, for example, the tag is placed into a pocket. The system will only restart when there is a sufficient light level for communication and solar charging extending the lifetime of the device. The system was designed to provide uplink and downlink data rates of 100-1000 and 10,000 bits per second respectively, over several meters.

The applications for such a system could include keyless access and industrial monitoring. An example being the positioning of goods or people around a factory along with the granting of access for users to areas or equipment.

This project has received funding from the European Union's Horizon 2020 research and innovation programme under grant agreement No 825651 (ELIOT)

5 Modulation Choice for Performance at Low Power

The following Chapters 6, 7, 8, 9, 11, 12, 13 address multiple aspects of the choice of the modulation method and compare various solutions. These chapter are excerpts from publicly available papers.

In recent research on optical wireless communication (OWC) systems, the focus normally has been on multicarrier modulation schemes. These have been cited for giving for high spectral efficiency, however as we argue in [6] there has been some confusions over this claim. We will address these in the context of power aspects. For instance, OFDM requires more linear, thus more power-demanding modulators. On the other hand, OFDM can better exploit an optimized spread of power over the modulation bandwidth (water filling), thus get the highest throughput for a given channel and a given power budget. OFDM wastes power as it may need a DC bias.

It can be argued that spectrum efficiency does not improve with OFDM. In fact, OFDM can be seen as an invertible matrix operation over the signal space. For OWC, it translates $N/2$ complex valued symbols into N real ones, thus preserves spectrum efficiency. However, it places symbols in narrowband frequency bins, such that the signal power and constellation can be optimized for each frequency. This differs from radio-wave communication, where the vast majority of standards only exploit bit-interleaved coded OFDM to retro-actively repair data lost on (typically) sharp frequency-selective multipath nulls, but do not allow pro-active adaptive bit and power loading in the transmitter.

Nonetheless, OFDM has distinct advantages for OWC. It can work well within the non-flat, low pass nature of optical components and channels that have to be loaded beyond the 3 dB bandwidth of the LEDs. State-of-the-art Radio Frequency (RF) networks broadly use multicarrier modulation in the form of OFDM, while some adaptations are necessary to make them work under the constraints of OWC channels, which require a non-negative and real-valued waveform. Some of the widely investigated candidate waveforms are DCO-ODFM, Flip-OFDM and ACO-OFDM [13]. OFDM, in particular DCO-OFDM, is a popular modulation method for LiFi as it can assign specific power levels and constellations to all frequencies in the low-pass response of the LED. However, the LED exhibits non-linearities to which OFDM is very sensitive. Yet this distortion is subject to intertwined memory effects and latencies in hole-electronic recombination in the semiconductor junctions. This colors the distortion and the extent to which input signals cause distortion also depends on the spectrum of the input signal.

Bit loading strategies that are suitable for LED communication, which remain simple in implementation and do not consume excessive power in signalling and signal detection, may offer significant improvements in performance. Compared to the existing techniques in G.9991 (G.vlc) it is to be investigated if non-uniform power allocation is useful in addition to the already used bit loading and if the bit loading has to be revised.

PAM-2 or On-Off-Keying allows efficient front-end design based on switching amplifiers (class D), which could reduce power usage by 1-2 orders of magnitude [14]. In addition, a higher average output power can be achieved for the same peak transmitter power due to a near ideal PAPR. In combination with wide field of view optics and link diversity, this overall more efficient use of transmitter power enables the design of very reliable optical networks. This is a critical advance for industrial deployment.

This project has received funding from the European Union's Horizon 2020 research and innovation programme under grant agreement No 825651 (ELIOT)

Moreover, results indicate that PAM with uniform signal levels can outperform OFDM as the latter is hampered by its Gaussian amplitude distribution. In fact, the OFDM backoff to accommodate a large peak-to-average ratio) PAPR is about 10 dB, and this can be much lower for PAM. This gives an immediate gain in SNR. Admittedly, channel equalization for PAM comes at a penalty either in transmit backoff (e.g. to accommodate a pre-emphasis) or as a noise enhancement, but may outweigh the disadvantages of OFDM, with jeopardizing spectrum efficiency.

5.1 Modulation for a low-pass channel

In short, we see that for communication over LEDs, OFDM is attractive to exploit the low pass nature of the LED (thus get more throughput for same effectively emitted power, see chapter 7), while PAM is attractive to build power efficient modulators (see chapter 6).

To handle the low-pass nature of LEDs, Orthogonal Frequency-Division Multiplexing (OFDM) adapted for optical applications (denoted as Optical OFDM, O-OFDM) is popular. In fact, O-OFDM allows to optimize the distribution of the available modulation power among the sub-carriers and to select the bit loading independently on every sub-carrier to maximize the data rate. However, the OFDM waveforms have a highPeak to Average Power Ratio (PAPR), making a large DC bias necessary to accommodate negative peaks in the signal. OFDM also requires highly linear (Class A) amplifiers, which are inefficient. In an OWC link, a pre-emphasis filter can be used in front of the LED to flatten the channel frequency response. In this case, using the simpler PAM modulation with lower PAPR instead of OFDM would reduce the required bias, and thus the drained power.

Depending on the application, the constraint from the channel differs. For VLC, the DC power is already available for illumination and modern LEDs are designed to havea high wall-plug-to-lumen efficiency. However, modulation costs extra electrical power that can deteriorate the overall system efficiency and has to be limited. Thus, for VLC, *extra* consumed power is the key constraint, rather than total electrical power. Particularly for IR, the human eye safetycan limit the average optical power to be transmitted by the LED.

To have a fair comparison of PAM and DC-biased Optical OFDM (DCO-OFDM) under certain constraints, one needs to operate both systems at their particular optimum. A proper framework includes for OFDM:

- optimum sub-carrier–dependent bit and power loading,
- optimized total bandwidth, and
- optimum bias current and modulation depth, in relation to the optimally tolerated clipping level, considering a realistic non-linear LED model (clipping, static and dynamic higher–order terms),

for PAM:

- pre-emphasis, with associated back-off to adhere to the power constraint and
- optimum constellation, we see that for the LED channel, the optimum does not necessarily lie at the smallest constellation (e.g.2-PAM),
- optimized bandwidth, which may deviate from the LED bandwidth.

This project has received funding from the European Union's Horizon 2020 research and innovation programme under grant agreement No 825651 (ELIOT)

For both modulation methods bandwidth and modulation order, in contrast to non-dispersive AWGN channels, addresses

- the type of (extra) electrical or optical power constraint imposed by the application, and
- the low-pass LED response.

The comparison of different modulation schemes was studied extensively. In fact, with respect to the above listed aspects, previous papers known to us lack at least one aspector do not generalize their findings into generic throughput expressions that extend beyond the simulation range of many previous papers.

DCO-PAM, thus level-shifted, non-negative PAM was shown in [15] to outperform all variants of OFDM in terms of optical power efficiency (including DC bias power) over a range of spectral efficiencies. Numerical optimization for a constrained peak optical power in [16] showed that in a limited bandwidth, DCO-PAM performs better.

In DCO-OFDM, the modulation depth, relative to the DC- bias determines the amount of clipping. This may prohibit the use of larger modulation orders. In [16], clipping noise was assumed to have a flat spectrum at the receiver over all FFT outputs regardless of the actual signal bandwidth. However, we show that the clipping noise predominantly depends on the modulation bandwidth. That is, one cannot arbitrarily spread clipping noise outside the signal bandwidth by using faster, oversized FFT processing at the receiver. Moreover, the clipping artefacts further are subject to the low–pass LED frequency response.

The work in [17] compares single–carrier (but frequency– domain equalized) M-PAM modulation to multiple OFDM variants, with a main focus on multi-path dispersion of the OWC propagation channel. M-PAM appeared to require alower SNR to achieve the same Bit Error Rate (BER). Both LED clipping and low-pass memory effects are covered in numerical simulations. However, no further optimizations for modulation bandwidth nor for a (frequency–adaptive) modulation order are discussed. On-Off Keying (OOK) shows a better optical power efficiency than DCO-OFDM and unipolar Asymmetric Clipped Optical OFDM (ACO-OFDM) in single-mode fiber systems [15], where the DC bias and bandwidth optimizations were carried out by numerical simulations, considering clipping for low biases. We further study ACO-OFDM in Chapter 13. At low available transmit power, ACO-OFDM can become more attractive than DCO-OFDM. However, for the same power, PAM reaches higher throughput.

In [18], OFDM has been studied for VLC in flat and dispersive channels, addressing also clipping noise while optimizingthe DC offset of OFDM. However, the practical limitations of a discrete modulation order (see chapter 14.1) and an optimization of the modulation bandwidth for OFDM were not discussed (This Chapter). On a pre-emphasized channel, the use of a fixed number of constellation bits over a fixed (non-optimized) bandwidth causes pronounced, abrupt discontinuities in the throughput, versus changes in the SNR [8]. That is, e.g., if the receiver gradually moves away from the transmitter, there will be a stepwise, non-graceful cut-off in throughput. In [19], throughput achieved by OFDM-based schemes were discussed. The clipping noise as well as the distortion introduced by the LED are

This project has received funding from the European Union's Horizon 2020 research and innovation programme under grant agreement No 825651 (ELIOT)

modelled. However, the results of [19] did not include the frequency selectivity of the LED channel. In ELIOT we studied the combined effects of a lowpass and distorting LED (Chapter 9).

To optimize OFDM for frequency selective LED channels, different power and bit loading strategies have been discussed in the literature, e.g. [8], [20, 21, 22, 23, 24, 25]. Waterfilling and uniform bit loading (also known as pre-emphasized power loading) are the two well-known strategies. Waterfilling is known as the optimum strategy that results in the maximum throughput in a frequency selective communication channel [20]. However, it requires a (relatively) complex algorithm [8], [21], [22]. The existing ITU g.9991 standard [26] simplifies this into assigning the same power level to all sub-carriers, but adapts the constellation per sub-carrier. Forcing a uniform constellation on all sub-carriers would further simplify the implementation to a great extent [25]. This is also considered in the current standardization of IEEE 802.11bb [27], as it can reuse approaches designed earlier for RF channels. In this work both waterfilling and pre-emphasis strategies are considered.

Contributions of ELIOT work include:

- In many other communication channels, using a higher bandwidth enhances throughput. In contrast to this, we show that for an LED there exists an optimum modulation bandwidth beyond which the throughput reduces. Moreover, OWC standards that fix bandwidth, as radio standards typically do, abruptly fail to sustain a weakening link.
- To make a fair comparison among systems that optimize their transmit bandwidth, we introduce the Normalized Power Budget (NPB), defined as transmit power corrected for path loss, normalized to the noise in the 3 dB bandwidth of the LED. In fact, we cannot use the bandwidth of transmit signal as different modulation strategies optimize differently.
- We derive mathematical expressions for the throughput and the preferred modulation bandwidth for DCO-PAM and DCO-OFDM. Using the now commonly reported exponential OWC channel frequency response [28], [29] , we capture these in new expressions. Hitherto, the comparisons were mostly limited to simulations for specific settings, thereby did not give generic expressions for other settings. Furthermore, we derive expressions for the optimum modulation bandwidth for DCO-OFDM and for (DCO-) PAM, considering discrete modulation orders and optimizing for the LED low-pass response. Our optimization includes the impact of limiting the DC bias for an OFDM signal, by allowing clipping and by making a trade off with the resulting clipping noise.
- We quantify clipping for DCO-OFDM as it raises the perceived noise floor and thereby limits the usable modulation order, even in an otherwise noise–free channel. Following arguments in [8], [15], [18], [5], [30], [31], we conclude that for modern LEDs, a saturation peak limit does not accurately model the behavior.
- We compare constrained optical power (related to the average LED current), the extra electrical power (related to the variance of the current caused by modulation) and the total electrical power (related to a combination of DC current and AC variance, weighted by the LED (say, bandgap) voltage and the dynamic resistance, respectively). While previously published works, e.g., [15], [16], [17] often report clear preferences for the choice of modulation, we conclude that there is not always a simple unique answer to the question whether OFDM and PAM is performing better, depending on which constraint applies.

This project has received funding from the European Union's Horizon 2020 research and innovation programme under grant agreement No 825651 (ELIOT)

- We show that in a VLC context, where the extra power needs to be far below the illumination power, there is no difference in performance between pre-emphasized DCO- OFDM and a DCO-PAM. However, DCO-OFDM with waterfilling outperforms DCO-PAM. For IR, where the bias or the mean DC light has to be paid for from the communication power budget, PAM with an appropriate high-boost (i.e., a pre-emphasis) and a carefully chosen bit rate and bandwidth outperforms pre-emphasized OFDM. Our model of the impact of clipping artefacts allows us to optimize the choice of the modulation depth for OFDM. In fact, one can intuitively interpret our results as a quantification of the effect that the power penalty incurred for the DC bias in pre-emphasized DCO-OFDM is not compensated by the ability to adaptively load sub-carriers in a high NPB range. For high power budgets, with an NPB above 30 dB, however, we found that OFDM with waterfilling and optimum choice of LED bias current outperforms PAM. Here, OFDM can fully exploit the adaptive bit and power loading. For high power budgets one can afford a large back-off of the modulation depth to avoid clipping of the OFDM signal, the latter conclusion disagrees with [16]. We show that the crossover point where OFDM with waterfilling outperforms PAM moves to higher power budget values when LED is biased at higher currents. If, instead, more LEDs were used to boost coverage, this would not happen.
- We propose a simple rule of thumb and an algorithm to optimize the modulation order and the modulation bandwidth of M-PAM, which works for both VLC and IR applications.

5.2 Modulation for a non-negative channel

As we discuss in Chapter 13, we studied ACO-OFDM in [13] and contributed to the understanding of its performance. We enhance Flip-OFDM to ensure phase continuity at the transition from the first OFDM block into the second flipped OFDM block. This avoids the need for a Cyclic Prefix (CP) between the two OFDM blocks. Mathematically, this modification shifts all signals up in frequency by half the subcarrier spacing. This is also equivalent to applying a linear phase ramp up to reach a 180 degree rotation at the end of the first block. It makes the OFDM anticyclic, instead of cyclic. This modulation can be done by a simple multiplication with a complex exponential after the transmit IFFT. To prepare for this, we also replace the usual Hermitian-symmetric padding, which is commonly applied at the IFFT input in IM OWC transmitters, by zero padding and by using the resulting complex-valued signal after the transmit IFFT for this phase rotation. We then take the real part of the signal. Moreover, we show mathematically that due to the frequency uplift by half a subcarrier, CP-Flip-OFDM and ACO-OFDM are mathematically equivalent. This new insight leads to novel, less compute intensive processing of ACO-OFDM.

This project has received funding from the European Union's Horizon 2020 research and innovation programme under grant agreement No 825651 (ELIOT)

6 Equalized PAM and OOK

The hard switching between two or possibly more signal levels can be implemented more power-efficiently than the linear power amplifier needed for OFDM. This can give a motivation to use PAM or OOK.

The bit rate that can be achieved over a communication channel depends on the bandwidth B_w and on the signal-to-noise ratio SNR. LiFi links are mostly limited by the additive white Gaussian noise (AWGN) in the transimpedance amplifier (TIA) in the receiver rather than by Poisson (shot) noise. The use of the Shannon capacity formula for channels that are constrained to non-negativity faces objections in the information theory community if used without justification. Therefore, we have derived a similar relation between throughput, the LED bandwidth and efficiency, signal bandwidth, and the logarithm of the SNR, and the rate achieved. This paved the way for making system choices.

6.1 Pre-emphasized PAM

An important aspect is the frequency response of the link and the penalty to achieve a bandwidth beyond that of the uncompensated LED. This penalty depends on the bandwidth used by the modulation method. For M-PAM, every symbol carries m ($M = 2^m$) bits in a Nyquist bandwidth of $f_{max} = r_s /2$, with symbol rate r_s and bit rate $r_b = r_s \log_2 M = 2f_{max} \log_2 M$.

We observed interesting effects, for instance on the impact of Increasing the constellation, at the same symbol rate.

- Going from 2-PAM to 4-PAM (doubling the number of bits per symbol from 1 to 2) at the same BER requires twice as many levels. The distance between levels should stay constant (to keep the same BER), 6 dB more power (4 times) needed to double the bit rate. This is more attractive than boosting the symbol rate, provided that f_{max} is far above the 3 dB bandwidth.
- Going from 4-PAM to 16-PAM (doubling the number of bits per symbol from 2 to 4), at the same BER requires four times as many levels as 12 dB more power (16 times). This is not attractive, compared to doubling the symbol rate.

This suggests that in a noise-limited LED system with first order roll-off, 4-PAM is about optimum, if the channel is a first order LPF. Yet the POF may give a steeper roll-off than first order.

6.2 Possible advances in PAM

6.2.1 Pulse Modulation and Frequency Domain Equalization

An interesting approach to address power saving is the use of a pulsed-modulation (PM)-physical layer (PHY) instead of OFDM [14] [31]. The IEEE 802.15.13 standard [32] defines three PHY modes, two of which are different configurations of OFDM systems and one is the PM-PHY investigated in ELIoT. In its simplest form the PM-PHY employs on-off-keying, which constantly utilizes the full modulation amplitude of the transmitter and thus can be expected to reduce energy and linearity requirements

This project has received funding from the European Union's Horizon 2020 research and innovation programme under grant agreement No 825651 (ELIOT)

on its power amplifiers. Line-coding and frequency-domain equalization (FDE) are employed to adapt to optical frontend characteristics and frequency-selective channels.

Since the PM-PHY is developed in the context of the IEEE 802.15.13 standard, these timings are adapted to the high bandwidth (HB)-PHY from the same standard for better compatibility, which in turn is based on the OFDM-based communication standard G.9960 and its derivative G.9991, specifically aiming at OWC [33], [26].

6.2.2 Performance of PM-PHY with Frequency Domain Equalization

To evaluate the performance of the PM-PHY for LiFi, a several measurements and detailed simulation have been performed in [14] [31]. These measurement results show that the transmission of signals according to the PM-PHY defined in the IEEE 802.15.13 standard across distances up to 5 meters are feasible with high-bandwidth frontends. While there is some potential for optimization in the transmission of the header data, the general concept based on 8B10B, Reed-Solomon FEC, and frequency domain equalization is shown to be applicable to real-world transmissions.

6.2.3 Line-coding, 8b10b and beyond

The measurements above applied an 8b10b line coding scheme to overcome the high-pass characteristic of the optical frontends. Other approaches to remove the DC component from on-off keying-modulated signals of the pulsed modulation PHY (PM-PHY), which is a physical layer for optical wireless communications that enables the use of switched mode transmitters, and thus promises significant energy savings were investigated in [34]. The results show the potential of 64b67b line coding as an optional high-speed mode to the PM-PHY specification in IEEE P802.15.13.

This project has received funding from the European Union's Horizon 2020 research and innovation programme under grant agreement No 825651 (ELIOT)

7 Optimizing Optical OFDM: Power and Bit Loading

This study is publicly available as [7]. One main conclusion is that uniform power loading, but with an adaptively chosen maximum frequency is as good as water filling. However, if an integer number of bits is loaded, uniform power loading may lack 1.5 dB of performance.

7.1 Modelling OFDM throughput and “capacity” formulas

For modulation beyond the LED bandwidth, preferably OFDM is used to optimize the modulation for each frequency bin. In fact, OFDM rotates the footprint of data symbols in the time-frequency domain by applying an inverse Fourier Transform (FT) on the sequence of incoming symbols [35]. The FFT is a unitary (invertible) matrix operation over complex number. To ensure an invertible operation by an *N*-sized FT and a real-valued output, the input of the FT is limited to N degrees of freedom, more precisely *N*/2 QAM symbols. Despite claims made in several papers, OFDM does not change the spectrum efficiency, as it uses all available dimensions in the time frequency plane and cannot create more dimensions (Nyquist theory holds for any signal). A Fourier transform operation with Hermetian-symmetric complex inputs and real-valued outputs converts *N*-symbols in into *N* symbols out. This operation is invertible, which confirms that OFDM preserves spectrum efficiency and that it is equally spectrum efficient as PAM. The advantage of OFDM lies in its ability to allocated power and constellations in a way that is optimized for the low pass nature of the LED [36, 8].

If the received signal power increases, OFDM can not only use and increase signal strength per subcarrier, but it can also use more subcarriers by using a wider bandwidth, typically far beyond f_{LED}. Figure 4 illustrates that at higher powers, the system can both use denser constellations (higher *M*, more bit/s/Hz) and use higher modulation frequencies.

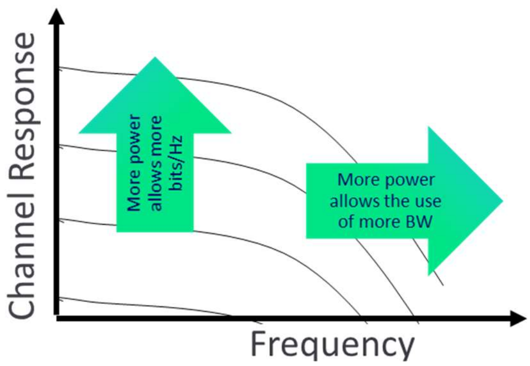

Figure 4: Channel response versus frequency.

Figure 4 shows the channel response versus frequency, at subcarrier frequencies where the signal is sufficiently above the noise floor, bits can be loaded on corresponding OFDM subcarriers. Increasing the received power lifts the response curve and enables not only more bits on already used subcarriers but also allows the use of more (higher) frequencies.

Particularly above f_{LED}, the signal-to-noise ratio is frequency dependent: the system can optimize its signal power distribution of the frequency domain.

This project has received funding from the European Union’s Horizon 2020 research and innovation programme under grant agreement No 825651 (ELIOT)

A key aspect of [7] is the trade-off between choosing LEDs which have a large f_{LED} versus LEDs that are optimized for efficiency. We argued in [7] that the use of a signal-to-noise ratio is less appropriate as it depends on the frequency, thus on spectral power density, not only its integral (total emitted power). We conclude that although may reviewers challenge the use of Shannon-like expressions for the throughput of DCO-OFDM, there is a solid justification for the use of a throughput expressed as an integral of the logarithm of one plus a weighed SNR.

7.2 Review of Power Loading Strategies

Water-filling is known as the optimum strategy for loading power on every OFDM subcarrier. That is is minimizes the power needed to achieve a certain bit rate. However, its implementation causes additional computational complexity, which introduces power consumption. Alternatives with low computational complexity are the uniform and pre-emphasis bit and power loading strategies [37, 7], for which their performance is to be investigated.

Figure 5(a) shows the typical LED response with gentle roll-off. Using the three different strategies, the transmitted and received power spectral densities are illustrated in Figure 5(b) and (c), respectively. For water-filling, we observe that, at least for low frequencies, the transmit power also exhibits a gentle roll-off, which is illustrated in Figure 5(b). The power spectrum that falls on the receiving detector follows the channel frequency decline shown in Figure 5(c).

Uniform loading transmits the same power on all frequencies but adapts the constellation, while the pre-emphasized power loading transmits the same number of bits per sub-carrier but adapts the power to invert the channel attenuation. These two practical strategies also appear to be relevant to current standardization, in particular to ITU G.9991 and IEEE 802.11bb, respectively. In fact, commonly used implementations of the ITU G.9991 (or G.vlc) standard apply a uniform power loading. Chipsets have been designed for communication over cables (mainly power lines), where the main constraint is the Power Spectral Density (PSD) which is constrained to satisfy electromagnetic interference (EMI) regulations. Alternatively, the IEEE 802.11bb effort tends to opt for reusing its legacy PHY, which was designed for radio systems that do not use adaptive power loading. It is well known for RF that deep fades are narrow as the multipath propagation has a sufficiently long delay spread (thus a small coherence bandwidth), so the frequency selectivity can in RF be overcome by appropriate error correction coding based on redundancy and bit-interleaving an using a fixed constellation on all frequencies. Yet, when used over an LED channel, adaptive bit-loading is needed as wide portions of the channel are heavily attenuated.

This project has received funding from the European Union's Horizon 2020 research and innovation programme under grant agreement No 825651 (ELIOT)

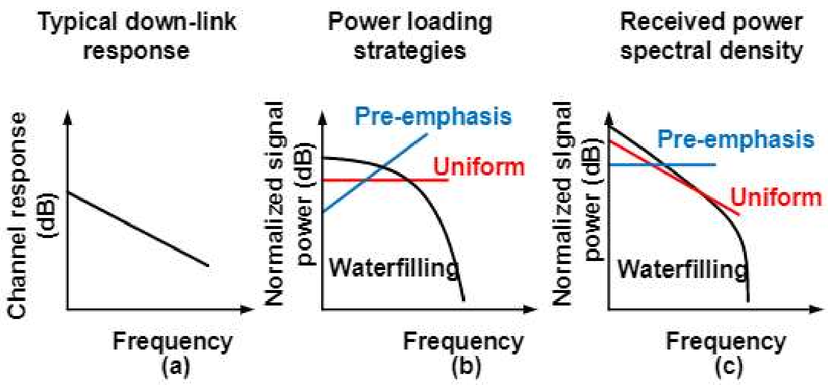

Figure 5: Illustration of the different power loading strategies [37].

Figure 5 illustrates the different power loading strategies with: (a) channel response, (b) allocated power versus frequency and (c) PSD at the output of the LED for water filling, uniform loading and pre-emphasis [8].

7.2.1 Optimized power and bit loading

Based on a theoretical Lagrange optimization, Water filling algorithm choses the optimum number of bit/s/Hz in accordance with the SNR of the various frequency bins. The iterative Hughes-Hartogs (HH) loading algorithm approaches this theoretical result, in practical implementation, including the effect that only discrete constellations are used with an integer number of *m* bits per subcarrier. The constellation size *M* is $M = 2^m$, where *m* is an integer.

HH starts with a known frequency response of the channel and a known noise spectrum. That is, it assumes that it can calculate how much power is needed on a particular frequency to transfer a particular number of bits per symbol. The algorithm iteratively searches for the most effective, i.e., least power consuming subcarrier frequency to transmit one more bit in the OFDM frame. In every iteration, it calculates the power penalty for increasing the constellation size. In fact, adding one more bit in a particular signal dimension requires a doubling of the constellation size, thus, say a 6 dB (or 3 dB) larger signal power.

At low frequencies, where typically constellations are already large and carry several bits, adding one more bit requires an exponentially growing power investment. On the other hand, at higher, more-attenuated frequencies, the signal is attenuated more, thus higher transmit power may be needed already at small constellations. The algorithm may also decide to start modulating higher frequencies beyond the set of subcarriers that were already assigned in previous iterations. It then assigns the extra bit to the subcarrier frequency with the lower power penalty to achieve this extra bit of payload. It then does a next iteration for the next bit to be assigned. It iterates until the total power budget is consumed.

This project has received funding from the European Union's Horizon 2020 research and innovation programme under grant agreement No 825651 (ELIOT)

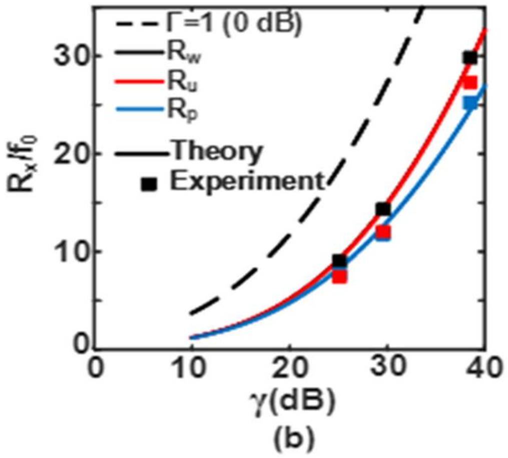

Figure 6: Bit rates by water filling, uniform loading with optimized, adaptive bandwidth and pre-emphasis

Waterfilling via HH is regarded as a relatively compute-intense solution. Typically, waterfilling solutions invest less power at highly attenuated subcarriers, thereby under-performing higher frequencies. This is thus in sharp contrast to pre-emphasis, that invests most power on underperforming subcarriers. Yet we see that the waterfilling solution gives an almost uniform power over a certain frequency band.

7.2.2 Uniform loading

The ITU G.9991 standard is mostly operated to use uniform power loading up to frequencies of f_{high} = 100 MHz.

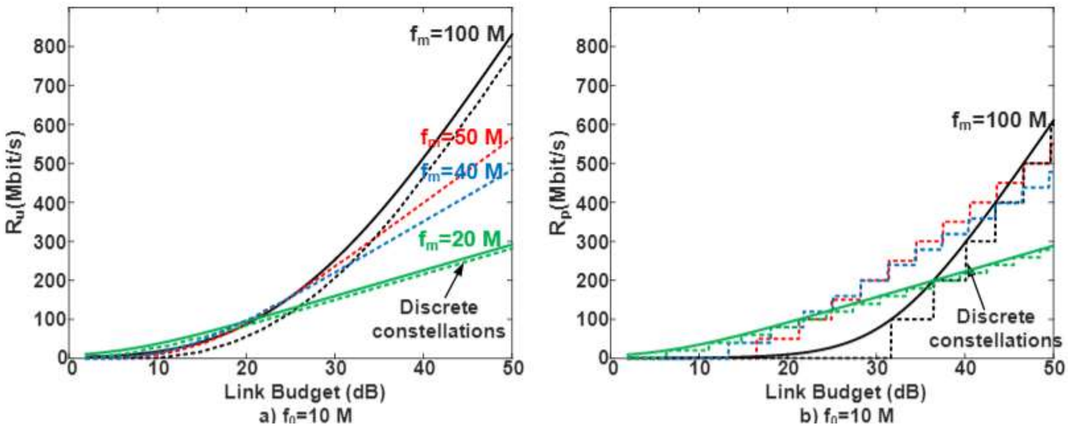

Figure 7: Achieved bit rates for an LED with 3 dB bandwidth of 10 MHz, using uniform power loading (left) and pre-emphasis (right), for various bandwidths f_m.

This project has received funding from the European Union's Horizon 2020 research and innovation programme under grant agreement No 825651 (ELIOT)

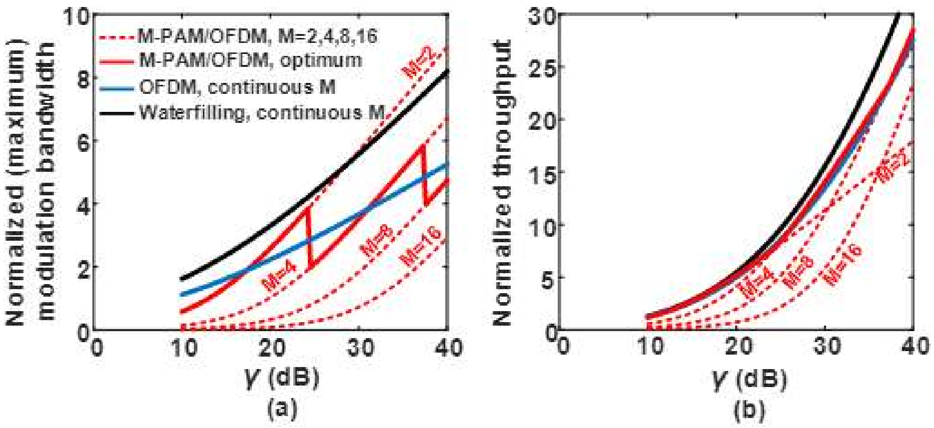

Figure 8: (a) (Optimum) normalized modulation bandwidth, (b) normalized throughput versus NPB used for modulation.

Figure 8(a) depicts the (Optimum) normalized modulation bandwidth ($f_{max_{PAM}}/f_0$, f_{max_p}/f_0, f_w/f_0 for PAM, pre-emphasized OFDM and waterfilling respectively) and Figure 8(b) shows the normalized throughput versus NPB used for modulation, γ, ignoring DC-bias power (VLC scenario). Dashed-red lines represent the performance for various constellation sizes M (for PAM and pre-emphasized DCO-OFDM) with the solid red being the choice of M optimized for maximum throughput. Solid blue and black lines represent the performance of OFDM with pre-emphasis and waterfilling, respectively, for continuous modulation order. For all plots $BER_M = 10^{-4}$

The figures seemingly suggests that the choice of power loading does not matter so much. But this is a bit misleading. There are a number of points to note

1) Uniform power loading performs equally well as the optimum water-filling only under a simplifying assumption that one can select a constellation of an arbitrary size. In practice QAM is used with an integer number of bits, (M-QAM, with M =2, 4, 8, 16, 32, 64, 128, 256, ..) or even an integer number of bits per dimension, (square M-QAM constellations, with M = 4, 16, 64, 256, ..). These round-off the number of bits per subcarrier and make 3 or 6 dB steps in effectively using the SNR. Thus, on average, uniform power loading wastes 1.5 to 3 dB in SNR. However, in this document we show how this loss can be repaired.
2) Waterfilling automatically selects an optimum bandwidth. In the plot, we assumed that the uniform loading and pre-emphasis also adaptively optimize their bandwidth. In some practical system this is not the case. As we will see later, choosing a fixed bandwidth comes with a severe penalty in bit rate. Particularly, in pre-emphasized systems, the throughput at low SNRs even collapses to zero.

This project has received funding from the European Union's Horizon 2020 research and innovation programme under grant agreement No 825651 (ELIOT)

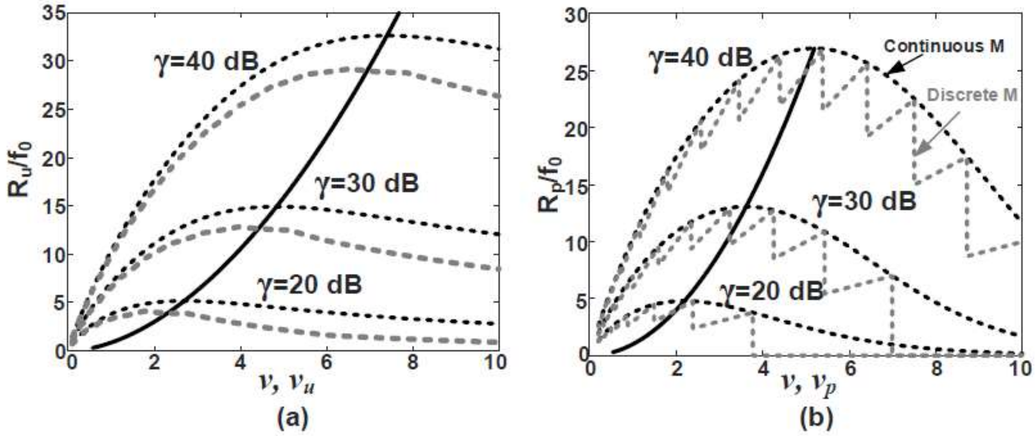

Figure 9: a) Throughput of OFDM for uniform loading, b) Pre-emphasis, as a function of bandwidth ν used [37].

Figure 9a) depicts the throughput of OFDM for uniform loading and Figure 9b) the pre-emphasis, as a function of bandwidth ν used. Bandwidth is normalized: ν is defined as the signal bandwidth in Hz divided by the 3 dB bandwidth of the LED f_0. Throughput R_u and R_p are also normalized to the LED 3 dB Bandwidth f_0. The solid line shows the optimum for maximum rate, which requires an adaptive choice of BW.

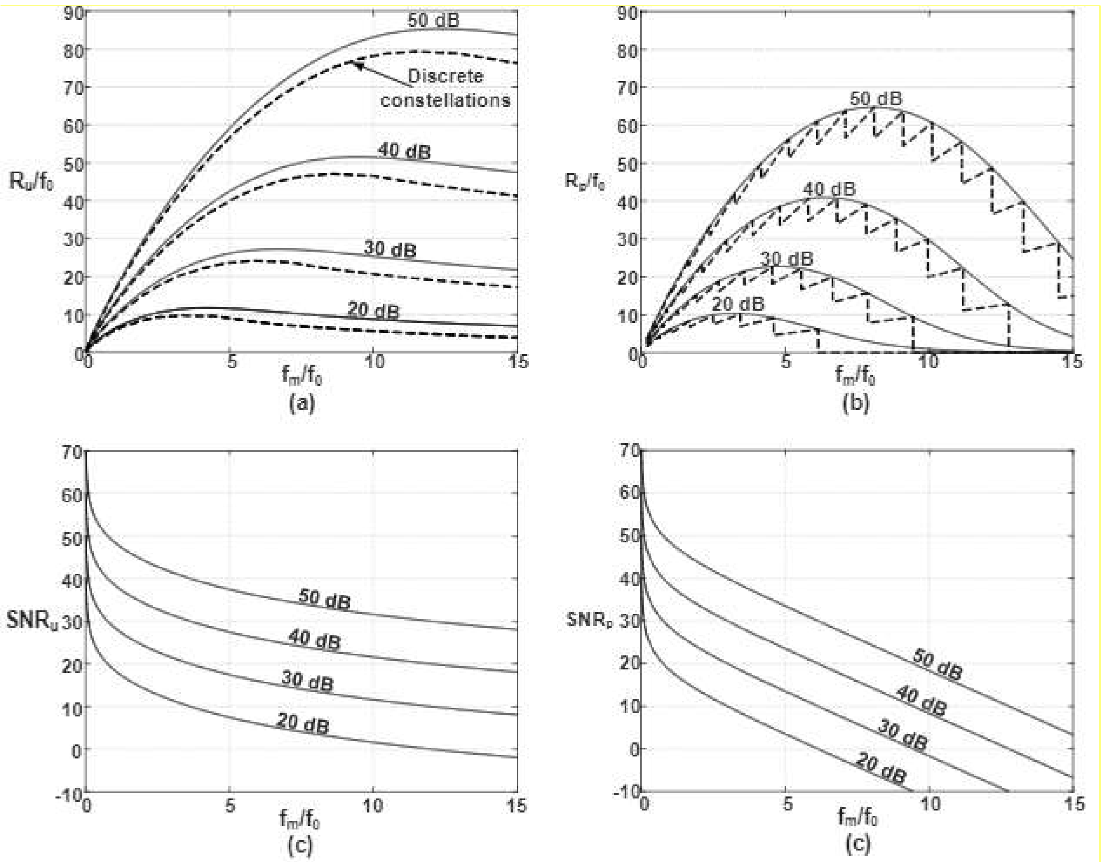

Figure 10: (a) and (b): Bit Rate (normalized to the LED bandwidth) as a function of the modulation speed. (c) and (d): Signal to noise ratio that is associated with the bandwidth used (for a given noise power spectral density and a fixed LED bandwidth).

This project has received funding from the European Union's Horizon 2020 research and innovation programme under grant agreement No 825651 (ELIOT)

The figures in this section and in the next section show the resulting bit rates for an optimal power loading and the fixed-bandwidth uniform power loading as typically used by early chip implementations of ITU G.9991 that reuse components oriented to wired transmission.

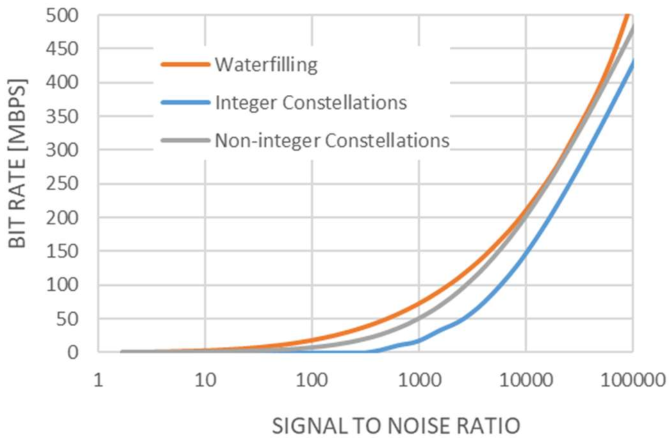

Figure 11: Adaptive bit loading in OFDM and Bit rates achieved

Figure 11 depicts the bit rate achieved with adaptive bit loading in OFDM by an ITU G.9991 LiFi standard-compliant chipset if operated with a uniform PSD up to 100 MHz, compared to the hypothetical use of constellations with non-integer number of bits per dimension, and to optimized power loading water filling.

7.2.3 ITU G.9991 vs IEEE P802.11bb

These two practical strategies (uniform power and pre-emphasis) also appear to be relevant to the current debates in standardization, in particular in ITU g.9991 and in IEEE P802.11bb. In fact, the recently released ITU g.9991 (or g.vlc) allows the use of adaptive power loading. However, early implementations of this standard apply a uniform power loading over large parts of the spectrum, with an adaptation of the constellation size per subcarrier. In this way, these implementations can reuse chip sets that already exist for communication over a power line, where the main constraint is the Power Spectral Density (PSD), typically requiring the same power on all subcarriers to satisfy EMI regulations. In fact, PLC uses the mains wiring, which typically leads to unwanted radiation of the signals. As these regulations prescribe different tolerable emission spectra on different bands, a specific spectral mask is prescribed that adapts this uniform PSD depending on the frequency range, thus deviating from a uniform PSD in some frequency ranges where more stringent requirements apply.

The algorithm then dynamically assigns more or fewer bits to each subcarrier. The system is robust against low pass filtering by the LED and / or optical indoor multipath by assigning fewer bits at high frequencies.

Alternatively, IEEE P802.11bb tends to opt for reusing its legacy Physical Layer (PHY), which was designed for RF radio systems that do not require adaptive power loading. In fact, deep RF fades are rare and narrow in radio multipath reception. This is particularly the case with a sufficiently long delay spread. So, the approach is to overcome fades by appropriate error correction coding, combined with

This project has received funding from the European Union's Horizon 2020 research and innovation programme under grant agreement No 825651 (ELIOT)

interleaving, with a fixed bit constellation on all subcarrier frequencies. Yet, when used over an LED channel, this approach is not so effective, while adaptive bit-loading can more effectively guarantee adequate throughput. In fact, a pre-emphasis is needed to avoid the consequence that highly attenuated high frequencies force the system to use only small constellation sizes. Adaptive bit loading is more effective if wide portions of the channel are heavily attenuated

In Chapter 14, we address the challenge of how to effectively perform adaptive bit loading, not only the bit loading itself (which is well known), but also methods to communicate between transmitter and the receiver to negotiate which constellation used on the various subcarriers.

This project has received funding from the European Union's Horizon 2020 research and innovation programme under grant agreement No 825651 (ELIOT)

8 Optimized current density of the LED

As seen in the previous chapters, the link throughput of an LED based LiFi system highly depends on the LED power and on the bandwidth. This chapter has been inspired by the review question “what makes a good LED” and how can we optimize the choice of the LED to reduce power. This chapter reproduces results reported in

- “Performance indicator of LEDs used for LiFi communication” by Jean-Paul Linnartz, Christoph Hoelen, Paul van Voorthuisen, Thiago Bitencourt Cunha, Haimin Tao, Amir Khalid, SPIE Photonics West 2022 [12]
- “Throughput optimization for IR-LEDs in an optical wireless link”, at ICC 2022

These papers build a model for the benchmarking and the selection of a suitable LED for LC and review LED measurements and theoretical models for such trade-off and applies these into communication bit-rate throughput expressions.

The design of well performing LED communication systems requires many design choices. Optimization of the LED itself and of the operational regime, e.g., the current density at the junction [38, 39, 40, 41, 42, 43, 44, 1, 45, 30], but also the choice of modulation, e.g., Pulse Amplitude Modulation (PAM) or Orthogonal Frequency Division Multiplexing (OFDM), the constellation (the number of bit/s/Hz), coding and a strategy to exploit bandwidth beyond the LED 3 dB bandwidth are topics of research. We refer in particular to [4, 3, 46, 47, 8, 7] for details on models and derivations that we will use in this chapter.

The design of an OWC communication system has a number of aspects that differ from RF systems. A radio link has to operate in a given, limited channel bandwidth according to regulations. In contrast to this, the LED acts as a low-pass filter but is not strictly limited in bandwidth. Hence, the signal to noise ratio is only given by the transmit power available, the pathloss, the noise power spectral density and by the choice of the signal bandwidth. This bandwidth is the subject of optimization thus shall not be fixed. This challenge has been addressed in the previous chapters.

This chapter (and paper [12]) adds another angle: the performance of the LED, in particular the bandwidth and the efficiency, which are both highly dependent on the current density [38, 39, 40, 41, 42, 43, 44, 1, 45, 30]. Increasing current densities helps to reduce the rise time and thus improving the modulation capabilities of the device, albeit at the cost of lower absolute output power [39]. In contrast, low current density helps to increase the absolute output optical power, which allows an increase in the illuminated area or an increase in the communication distance, but at the cost of a lower modulation bandwidth [39]. To explain the efficiency droop with increasing current densities, many mechanisms have been proposed in the literature. Of these, Auger recombination and carrier leakage are the most popular [40, 41]. Increasing the LED chip size [43], i.e., reducing the current density, may help diminish carrier leakage, but has an adverse effect on the thermal performance of the device [40]. It is known that increasing operating temperature deteriorates the device performance due to thermal droop [40]. Thermal management is then important to improve performance, but the use of thermal conduct sub mounts and large heat sinks increases device size and its manufacturing cost.

This project has received funding from the European Union’s Horizon 2020 research and innovation programme under grant agreement No 825651 (ELIOT)

Given a certain power budget, the system designer can choose the current density through the LED [42, 39]. One specific LED has a fixed die area, so the current density grows with the total LED current. However, we can take the die area as a degree of freedom and set the total current as a constraint to fairly compare systems with the same power consumption. By changing the die area, the current density changes.

For communication systems, the trade-off between bandwidth and effective power output directly affects link performance and what is an optimal design. The values chosen for communications also affect device efficiency and power consumption. These issues are investigated in the following sections.

The trade-off between efficiency and bandwidth was addressed experimentally for micro-LEDs in [42].This publication also hypothesized a power-law relation between bandwidth and effective power output of the LED. In the following sections we search for a theoretical justification of this model. We also connect it not only to pulse modulation within the LED bandwidth, but also to optimized and practical choices for the modulation method, the commercially used ITU G.9991 standard in particular.

8.1 Empirical LED Communication Model

In the choice of the operation of the LED, there is a trade-off between the power emitted and the LED bandwidth f_{LED}. Inspired by experiments reported in [38], we model this trade-off by

$$\eta_{TX}^{\alpha}\, f_{LED}^{1-\alpha} = C_{LED,1} \tag{1}$$

where C_{LED} is a system property. For GaN micro LEDs, [42] measured and curve-fitted the optical power versus bandwidth from GaN micro LEDs between 0.8 and 2.2 milliwatt and bandwidths of 90 to 200 MHz. Such micro-LEDs are mostly driven quite deeply into the droop region, thus far beyond the maximum quantum efficiency point. The bandwidth appeared to have a 1.67 times higher exponent than the LED power. Trade–off between power efficiency and exploiting bandwidth for PAM

As a first evaluation of the consequences of this model, we compare the LED operational regime, which allows a choice of bandwidth and power over a straight line on a log-log curve as in Figure 12.

This project has received funding from the European Union’s Horizon 2020 research and innovation programme under grant agreement No 825651 (ELIOT)

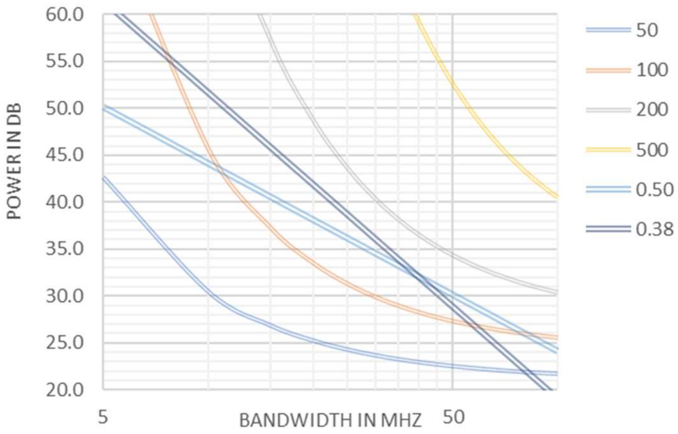

Figure 12: LED performance (doubled lines) and iso-bit rate curves (single lines), i.e., curve at which a particular rate is achieved by a well-chosen combination of power and bandwidth

Figure 12 depicts the LED performance (doubled lines) for α = 0.38 (dark blue, =) and for 0.5 (light blue, =) and the iso-bit rate (single) lines based for 50, 100, 200 and 500 Mbit/s using the throughput expression for PAM with a Nyquist bandwidth that equals the LED 3 dB bandwidth. The optimal LED operational point is where the LED curve touches the highest throughput curve.

The PAM throughput expressions can also be plotted in this plane: a certain throughput can be achieved in various ways: the bandwidth can be traded for power by choosing the number of levels *M,* where *M* affects both the required bandwidth and required power. In Figure 12, we assumed *M* to be a continuous-valued parameter.

8.2 Theoretical Model

In our publication we compared different types of LED and for this the current density is a key parameter that affects both the bandwidth and the efficiency. However, also temperature effects need to taken into account. The efficiency of the LED reduces if its temperature goes up [41, 45, 46, 48]. Out of the input power P_T, a fraction 1-EQE is converted into heat. Further modelling of the effect of heat allowed us to match our theory with empirical data.

This project has received funding from the European Union's Horizon 2020 research and innovation programme under grant agreement No 825651 (ELIOT)

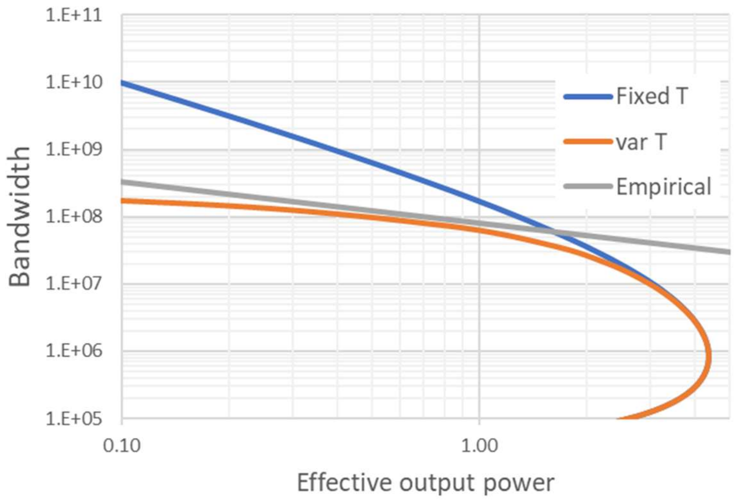

Figure 13: Optical modulated signal output power efficiency versus LED bandwidth

Figure 13 depicts the optical modulated signal output power efficiency η_{dEQE}versus LED bandwidth, for various choices of zeta thus for varying current density. Grey line: Empirical curve for micro-LED [42]; blue line: theoretical curve (ABC model) for OFDM and a fixed LED temperature of 25 C; orange line: Theoretical curve for an LED that heats up more if higher current densities are used.

Figure 13 compares empirical results in [42] (gray curve) with our results derived from the ABC model, with and without a thermal correction. Micro-LEDs operate at high bandwidths but lower effective power. Here the slope of the curve can be seen as fairly constant. Mid or high-power LEDs operate close to the maximum power and may not show very substantial droop effects. Here, driving a bit deeper into droop usually pays off as it significantly enhances the LED bandwidth.

Deep into the droop regime the α-law seems to be a reasonable model. However, closer to the maximum EQE thus closer to the bend in the curve, where most LEDs are operated, a substantial gain in bandwidth can be achieved without jeopardizing the power efficiency significantly. Nonetheless, we measured an alpha power law between WPE and bandwidth, as shown in Figure 13.

Table 2: Summary of studies into alpha-power rule of thumb.

	POWER EXPONENT	**BANDWIDTH EXPONENT**		
	α	$1-\alpha$		
GAN MICRO-LEDS FEHLER! VERWEISQUELLE KONNTE NICHT GEFUNDEN WERDEN.	0.38	0.62	$\eta_{TX}^{0.38}\ f_{LED}^{0.62}$	Increasing BW is associated with a larger change in power.
ABC FIXED TEMPERATURE HIGH CURRENT DENSITY	0.666	0.333	$\Phi^2 f_{LED}$	Deep into the droop regime. Relatively large improvement on BW if power is jeopardized
ABC AND TEMPERATURE CORRECTION, HIGH C	≈ 0.4	≈ 0.6		Increasing BW is associated with a larger reduction in effective power
MEASURED GAN LEDS AT 85 C	0.665 .. 0.727	0.335 .. 0.273		

This project has received funding from the European Union's Horizon 2020 research and innovation programme under grant agreement No 825651 (ELIOT)

8.3 Concluding remarks on LED current density

The bandwidth and the power, or power efficiency are key performance indicators for LEDs. However, there is not a straightforward way of expressing power and bandwidth into a single metric. In this chapter we presented a mathematical framework that evaluates this trade-off. This depends on many effects, including the modulation method and the way that the modulation adapts to bandwidth variations, and on the way that the temperature of the junction is stabilized.

Nonetheless, we see that a log-log relation: “efficiency to the power alpha x bandwidth to the power one minus alpha is a constant” works reasonably well. A key effect here is whether the temperature is kept constant via an active control or that just a heat sink is used such that the LED heats up more in less efficient regimes. For a fixed, e.g., active stabilized temperature, the alpha parameter takes on values of around 2/3, and it appears attractive to drive the LED quite far into a droop region to boost the bandwidth, even if this comes with some degradation of the efficiency. However, if the temperature of the junction will be higher if one allows lower efficiency and higher current densities alpha shrinks substantially and makes it less attractive to further boost the bandwidth. The latter, we saw in an earlier paper reported for micro-LEDs and was confirmed by our mathematical model. In particular, for micro-LEDs that are challenged in their output power, this may limit their suitability for long range links, where the received signal power is limited by path loss and efficiency counts.

Our SPIE paper developed a framework to link LED power to LED bandwidth. Via the choice of modulation, e.g., adaptive OFDM with variable bandwidth, the throughput can be optimized for the LED properties. It is then a further optimization on the optical design to link the output power to the coverage area, as we elaborated in a companion paper. From an application perspective, the bitrate-times-square-meters seems reasonable, as power grows linearly with the area covered (subject to design of the detector) but there is not a linear relation between bit rate and received power.

This project has received funding from the European Union’s Horizon 2020 research and innovation programme under grant agreement No 825651 (ELIOT)

9 Modelling non-linearity

Contents in this chapter are also reported publicly in the papers [7, 4]:

In the early days, e.g. [49], the LED was modelled as a peak limited channel. In fact, thermal breakdown of the semiconductor structure limited the maximum tolerable current. However, as solid-state lighting technology evolved, LEDs are no longer driven near their physical limits, but rather near their optimum efficiency, thus at far lower power levels. Increasingly, LED distortion is modelled as an invertible effect containing mainly second-order distortion that are invertible.

ELIOT used and extended the clipping noise model of [18] which considered one-sided clipping of the LED current. This extends our previous bitloading evaluations in [8], which assumed clipping-free DCO-OFDM, leading to more complete, realistic model.

Figure 14 (a) shows the PSD of 64-QAM (M = 8) on the 64 lower sub-carriers in an OFDM system with 128 sub-carriers thus with an IFFT size of 256. The PSD of the clipping noise is shown in Figure 14 (a) for $z = 0.5$ (overly aggressive clipping), $z = 1$ and $z = 2$, where we define a parameter z to be the ratio of the bias current over the LED rms current. This plot confirms our argument that the clipping noise is mostly confined within the modulation bandwidth of the signal where it may have two or three dB variations. Also, the clipping PSD raises with lowering z. For the signal in Figure. 2, $z \geqslant 2.2$ is required to achieve a simulated BER of $< 10^{-4}$.

Figure. 33(b) shows the minimum z as a function of number of bits per sub-carrier in one dimension for margins $r = 1$, 2 and 4. It can be seen that for a typical modulation order of 64-QAM (M = 8), $z \geqslant 2.15$ and $z \geqslant 2.4$ are needed for $r = 1$ and $r = 2$, respectively. Dashed lines in Figure. 33(b) also show the minimum required z for margin $r = 1$ for two values of α_2/α_1 when $I_{LED} = 0.3$ A. It can be seen that for modulation order of $M \leqslant 16$, thus 256 QAM, the minimum z (for this specific example) is dominated by the clipping noise and the distortion is negligible. Values in the range of a Signal–to–Distortion–and–Noise Ratio (SNDR) around 40 dB are achieved in commercial ITU G.9991 systems, allowing up to 1024-QAM ($M = 32$), or 4096-QAM ($M = 64$) at maximum. The steep dashed curves confirm the practical experience that modulation orders above $M = 64$ are hard to achieve at reasonable z. In future systems, the distortion may be overcome by a pre or post-distortion compensation method. Therefore, we do not elaborate on invertible distortion as limiting the throughput, so we focus on non-invertible clipping.

This project has received funding from the European Union's Horizon 2020 research and innovation programme under grant agreement No 825651 (ELIOT)

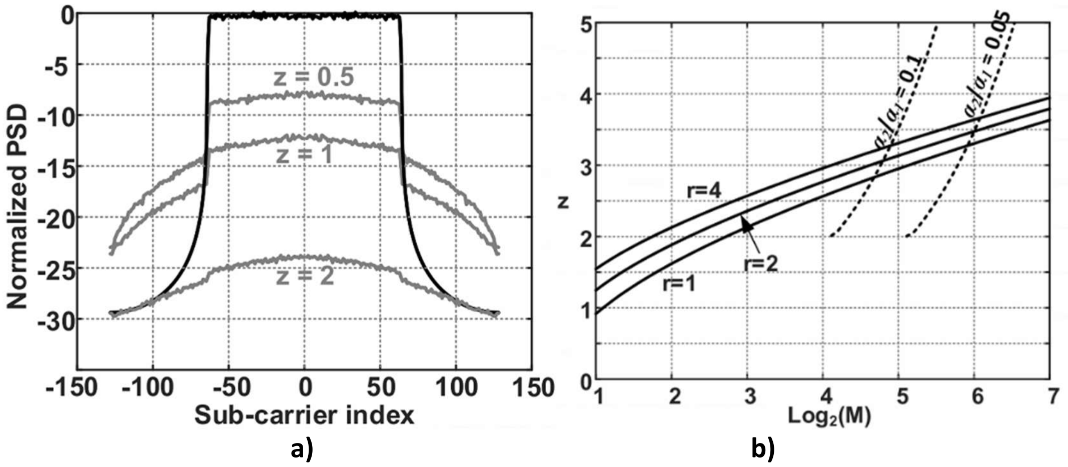

Figure 14: a) PSD of an OFDM signal; b) Bias ratio versus number of bits

Figure 14a) depicts the PSD of an OFDM signal (black) and clipping noise (grey), for bias ratio of 0.5, 1 and 2. LED low-pass response not included. Figure 14b) shows the bias ratio z versus the number of bits b = log2 M per sub-carrier in one dimension. The figure assumes noise-free reception (*r* = 1) such that no margin is needed for distortion and noise to add up and leaving a 3 and 6 dB power margin (*r* = 2 and *r* = 4, respectively) to operate over a noisy channel. Solid line: clipping limit. Dashed line: invertible distortion limit. For distortion–limited *z*, we used *r* = 1.

Our new insights show possible refinements, as the distortion is not an instantaneous, memory-less function of the input current. Models [50, 51] that cascade a distortion-free low-pass nature of the LED capacitance and static non-linearity may not adequately capture the effects seen in high-speed modulation, far above the -3 dB bandwidth of the LED. In fact, we observed that the distortion-noise is non-white, and depends on the input spectrum, as well as on the LED properties and its bias. Hence, the performance of an OFDM LiFi system is not well modelled by adding an elevated white (frequency-flat) noise floor. The distortion-noise differs per subcarrier, and different subcarrier loading strategies may be needed for distortion caused by LEDs. For the full report we refer to [4].

This project has received funding from the European Union's Horizon 2020 research and innovation programme under grant agreement No 825651 (ELIOT)

10 OFDM model for Distortion per subcarrier

We use rate equations of the semiconductor material to describe the electrical-to-optical LED response as a set of differential equations. This is used to give a non-linear continuous-time filter model. Inversion of the non-linearities has been studied and progress is made [2]. However, standard OFDM systems lack such interference elimination facilities. In the paper [4] we focus on the effect of distortion in an OFDM system that experiences interference as extra noise.

10.1 Single Frequency Sinusoid

For a single-frequency signal, the measured and theoretically modelled results are compared. Figure 16 depicts in solid curves the measured response (blue) to a sine wave current and second–order distortion (red) versus modulation frequency. The dashed curves reflect the results of the theoretical model, assuming an LED bandwidth of f_{LED} = 25 MHz and f_x = 7 MHz. X-axis in Figure 16 is the frequency of the fundamental.

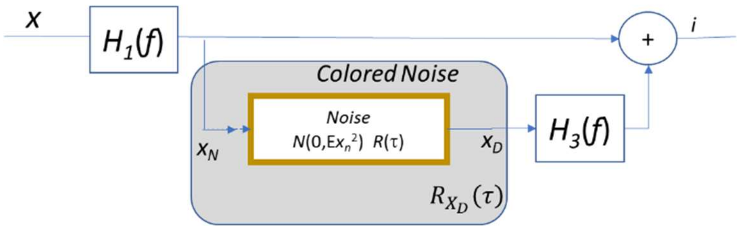

Figure 15: LED model for Distortion:
$H_1(f)$: low-pass linear response, $H_3(f)$: further shapes the distortion noise.

Above 50 MHz, the second order distortion is at above 100 MHz. However, the listed 3dB bandwidth of the Thorlabs PDA10A-EC Photodiode used for the measurements relevant to these results is 150 MHz. This explains why fundamental frequencies above 50MHz, thus with distortion above 100 MHz start to see lower distortion than theoretically predicted, with a 3 dB extra attenuation of distortion for a fundamental at 75 MHz.

This project has received funding from the European Union's Horizon 2020 research and innovation programme under grant agreement No 825651 (ELIOT)

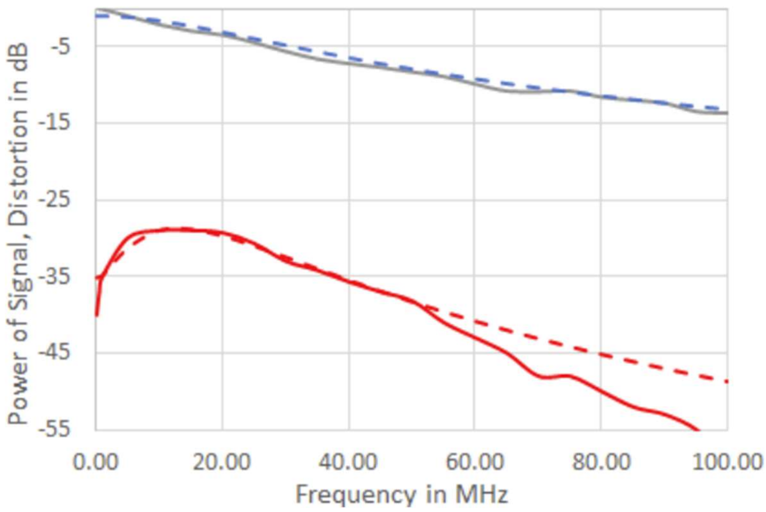

Figure 16: Power of signal and distortion versus frequency (measured and theoretical)

We see that the signal-to-distortion ratio SDR improves at high frequencies. Later we will see that this is in contrast to the situation for an OFDM signal where SDR deteriorates with frequency. For a single tone, the low-pass response of the carrier concentrations in the QW caused a reduction of the signal amplitude with frequency, thus distortion reduces twice as fast (in dB) with frequency.

We also see that at frequencies below the f_{LED}, the distortion also reduces. We explain this by introducing the concept of an "impatience penalty".

10.1.1 Impatience Penalty

The power of the distortion reduces with a second-order law above f_{LED}. We can give an intuitive explanation of why the distortion is lower for very low frequencies. In fact, at low frequencies the LED acts quasi-stationary. The different speeds at high and low currents do not affect the output, since the LED has time to adapt and reach steady state for both low and high currents.

We used a signal generator of type AFG3102: giving a 540 mVpp 20 MHz sinewave. The signal attenuation was set to 0 dB, which gave $\hat{I}_{Sine}$=150 mA, but the DC bias was changed I_{DC}=300, 200,150,100,60 mA. At I_{DC}=150 mA the minimum instantaneous LED current is 0 mA.

This project has received funding from the European Union's Horizon 2020 research and innovation programme under grant agreement No 825651 (ELIOT)

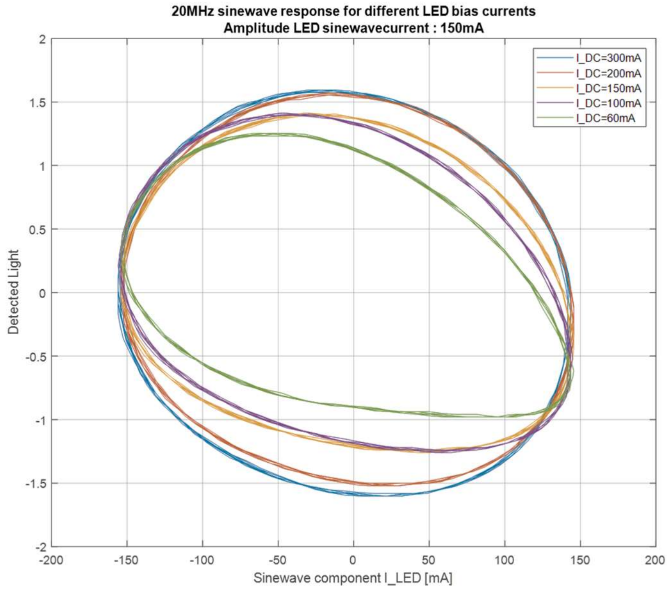

Figure 17: Sinewave response traces under different LED bias currents.

10.2 Distortion effects on OFDM

We modeled to what extent the distortion increases the noise perceived by typical receiver. We particularly consider OFDM.

For numerical analysis of the performance of OFDM, it is attractive to also have a model for distortion that can be used in expressions for the symbol or bit error rate (SER, BER). Unless dedicated signal processing is used to repair the non-linearities, the distortion acts as extra noise. In an OFDM system, such distortion is spread over many subcarriers. One may argue that on every time-sample, the probability distribution of a square of a Gaussian is not Gaussian but is chi-square (gamma) distributed. However, after the receive-FFT, many, typically a few thousand, samples are combined. That justifies the model of Gaussian distortion noise at the symbol detector in case of OFDM modulation, provided that we treat the DC term appropriately.

DCO-OFDM systems only work reliably with moderate amounts of noise, say 20 to 30 dB below the main wanted signal level. That is, assume mainly the first-order effect of non-linear operation on the wanted signal but neglect second-order effects of distortion being distorted further into higher order contributions.

In ELIoT we studied the spectrum of this noise in two steps, in particular because (1) the noise passes through the electro-optical system of the LED, which colors its response, (2) powers (here, mainly the square) of a non-white Gaussian signal are also colored, (3) a filtering experienced from QW to the light output.

Extending Bussgang's insight that distortion attenuates the signal and adds independent noise [52], we model this as in Figure 34. This allows us to consider effects that not the signal itself, but an H_1-filtered version of it is responsible for the variance of the noise. Secondly, H_3 allows us to model that the noise is non-white, and thirdly, H_3 reflects the fact that distortion does not directly hit the optical photonic output, but it is subject to an LED response as well.

This project has received funding from the European Union's Horizon 2020 research and innovation programme under grant agreement No 825651 (ELIOT)

10.2.1 Theoretical and Measured Results

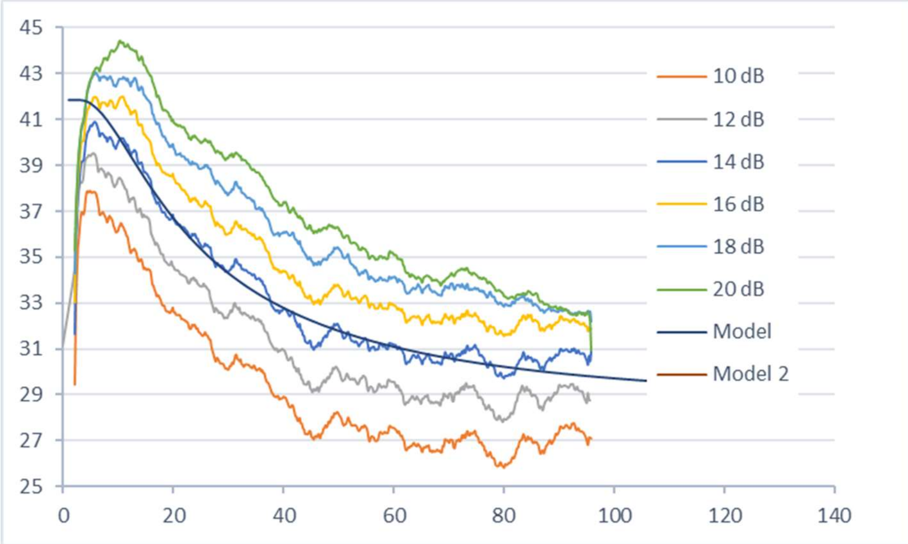

Figure 18: Measured and modeled Signal-to-Noise-and-Distortion Ratio SNDR for OFDM

Figure 18 depicts the measured Signal-to-Noise-and-Distortion Ratio SNDR for OFDM with a uniform power spectral density, for various attenuations of the modulating signal, and prediction by our theoretical mode.

We measured an OSRAM SYLVANIA LZ1-00R702 infra-red LED, biased at I_{DC} of 215 mA and modulated by an OFDM signal generated by a Maxlinear 88LX5153 Baseband OFDM PHY Integrated Circuit (IC) according to the g.9991 standard for LiFi (g.vlc). The system performance is mainly limited by distortion. The modulated signal was attenuated in the range 10 to 20 dB. The smallest attenuation of around 10 dB, gave a peak modulation of 205 mA, thus clipping was negligible. In fact, we positioned the Thorlabs detector such that LED signal is well above the detector noise while avoiding that detector also adds non-linear distortion. This is done by searching for a position where the MXL reports the same SNR values for a range of different distances between LED and detector.

In agreement with our expectation the signal-to-distortion ratio is the best if the attenuation is set to its highest value. For every dB of increased signal strength, the SDR deteriorates with exactly one dB. This confirms that the second-order distortion dominates. Third-order distortion or clipping would show a different relation.

At a frequency somewhere near the LED 3 dB bandwidth the SDR is best. This is in contrast to the case of modulation by a single tone, where the harmonic distortion was worst near the 3 dB bandwidth. We intuitively explain this as in an OFDM we consider distortion experienced at the subcarrier itself, thus distortion caused to other (e.g. double) frequencies with a flat power spectral density, a wide range of frequencies contribute to the distortion,

10.3 Sub Conclusions on LED Distortion in OFDM

Distortion has a limiting factor on the throughput of OFDM systems. To achieve high bit rates, large constellations are needed which are sensitive to the distortion. A first-order response may be to

This project has received funding from the European Union's Horizon 2020 research and innovation programme under grant agreement No 825651 (ELIOT)

reduce the modulation depth, but to reach an adequate coverage the system become limited by noise. This may then have to be compensate by emitting much more power.

This shows how combatting distortion, as we will do in Chapter 11, can save significant amounts of power. This section quantified the impact on power consumption.

This project has received funding from the European Union's Horizon 2020 research and innovation programme under grant agreement No 825651 (ELIOT)

11 Eliminating Nonlinearity

Contents in this chapter are also reported in:

> Mardanikorani, Shokoufeh, Xiong Deng, Jean-Paul MG Linnartz, and Amir Khalid. "Compensating dynamic nonlinearities in LED photon emission to enhance optical wireless communication." *IEEE Transactions on Vehicular Technology* 70, no. 2 (2021): 1317-1331.

LEDs have bandwidth limitations and exhibit nonlinearities [53, 30]. Multiple non-linear mechanisms, including imperfections in the LED electronics circuitry, contribute to the distortion of the IR or VLC signals. Effects in the LED junction itself typically are dominant [5]. Distortion due to the LED driver electronics, Digital-to-Analog Converters (DACs), Analog-to-Digital Converters (ADCs), Photo-Diodes (PDs) have been extensively studied in the past and can mostly be avoided [54, 2].

To repair LED-induced distortion, we start with a system identification via an appropriate LED model. Static nonlinearities were modeled in [52, 55, 56]. However, for high–speed applications using a large–signal bandwidth, the inclusion of memory effects in distortion can significantly improve performance, as the LED photon generation depends not only on instantaneous non-linear effects, but also on the build–up of hole–electron concentrations in the (recent) past [7], [12]. In this regard, Volterra series are very generic, thus can be applied for LEDs. However, this technique involves a large number of the parameters that all must be extracted and updated [7], [13], [14]. For example, for a Volterra series with a memory length N, N^p coefficients must be estimated for the pth kernel function. One needs an appropriate choice for the number of the memories taps and for the order of the distortion to avoid the use of an overly parameter-rich model. With a large set of Volterra parameters, its complexity makes Volterra series identification and distortion mitigation hard to implement for high-speed real-time applications. Nonetheless, we saw successful offline approaches in [57, 58]. LED models by Hammerstein and Wiener [51, 50] can be seen as an aggressively simplified subset of Volterra series. These models cascade a Linear Time-Invariant (LTI) low-pass filter with a separate memoryless non-linear block. However, [2] argues that such models fail to model the different fall and rise time constants. Moreover, eye diagrams show a level-dependent position of the optimum PAM sampling moment, which can be modelled only by considering non-linear operations on time–delayed signals.

In Chapter 8 and 9, models for the dynamic behaviour of LEDs have been refined in literature as the light output responses are described by non-linear dynamic differential equations [30]. We study the use of Double Hetero-structured (DH) LEDs. For this structure both the carriers and the optical field are confined in a central recombination region to achieve high optical efficiency. The ABC model for hole-electron recombination in the Quantum Well (QW) was used in [2, 59, 60] to describe the photon output as a function of the dynamic carrier concentrations. It can be extended to LED input–current–to–output–power relations. This method can model the LEDs with a lower computational complexity than generic Volterra approaches that lack a restriction to physical phenomena.

This project has received funding from the European Union's Horizon 2020 research and innovation programme under grant agreement No 825651 (ELIOT)

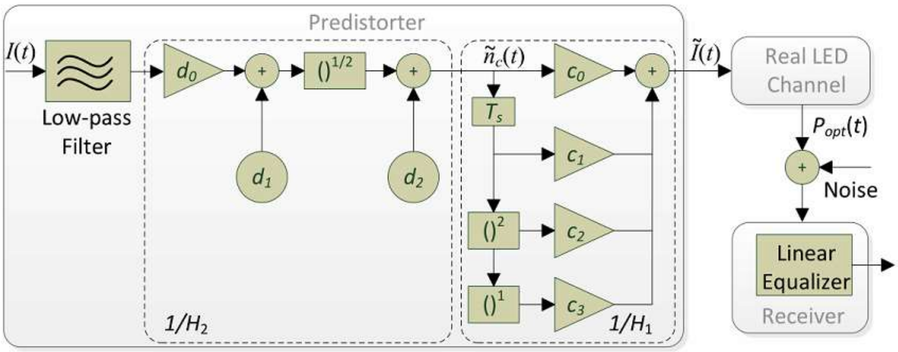

Figure 19: Proposed nonlinear predistorter for nonlinear LED channel.

Both the linear low-pass effect and the nonlinearity of LED are compensated by the predistorter. Theoretically, the predistorter can precisely shape the signal waveform to ensure the output of the LED is identical to the ideal signal, such that the LED bandwidth is unlimited. Such a predistorter exhibits a predominant pre-emphasis effect to invert the low-pass nature of the LED. This has practical disadvantages, for instance in the dynamic range of the amplifier and in controlling the LED modulation depth. A suitable approach can be to let the transmitter preserve the band-limited character in the LED channel, while the system can rely on known techniques to combat the ISI, e.g., linear or DFE discussed in Section IV (A) for PAM, or OFDM, possibly including adaptive bit loading per subcarrier. Figure 19 illustrates how a low-pass filter can be placed in front of the predistorter to preserve the LED high frequency fall-off. Commonly used equalizers can be then applied across this LED communication channel, in which non-linearities have been mitigated by the predistorer.

With the nonlinear predistorter, the bandwidth of the LED channel is limited by the low-pass filter. Based on the 3-dB bandwidth of the low-pass filter, the achievable data throughput in VLC can be analyzed along with the key system parameters such as the received SNR. The channel capacity also depends on the structure of the low-pass filter. For instance, a Gaussian low-pass filter results in a lower channel capacity than the first-order low-pass filter. This also gives us the insight to build the low-pass filter.

More information on the effectiveness of the predistorter in single-carrier PAM and multi-carrier OFDM can be found in our published paper in [2], and the information on the postdistorter at the receiver can be found in [59].

11.1 MMSE Nonlinearity Compensation

Full elimination of the distortion caused by the LED in a Zero-Forcing (ZF) manner, leads to excessive noise enhancements at the receiver, or excessively large high–frequency components in the LED driving signal. In [5], we study a Minimum Mean Square Error (MMSE)-based trade-off of noise enhancement versus minimizing residual distortion artefacts left at the receiver. Based on a pre–determined training sequence, the receiver estimates the equalizer parameters to minimize the total noise–plus–distortion power. LED parameter variations are caused for instance by aging, temperature drifts and different operating biases. As these do not change rapidly, parameter estimation is needed but does not need to be frequent so it may not necessarily impose significant additional communication overhead. The contributions of this manuscript can further be summarized as follows:

This project has received funding from the European Union's Horizon 2020 research and innovation programme under grant agreement No 825651 (ELIOT)

- Following the work in [59], we start with the physical model of photon generation and consider a discrete–time equivalent that can be inverted into a ZF non-linear equalizer. We modify this in two ways: We simplify the ZF structure to reduce the number of unknown coefficients from five to three, plus an overall gain parameter. We show that the model error stays well below the typical receiver noise floor.
- Secondly, we estimate the coefficients to minimise the Mean Square Error (MSE), also considering noise.
- For the simplified equalizer, we develop a model to study the effect of noise on the coefficient estimation and on the equalizer performance for random independent and identically distributed (i.i.d). Gaussian signals. Comparisons with the ZF approach are also provided. We show that the model results in a simpler set of equations for the estimation of equalizer coefficients.
- We show that the resulting, simplified equalizer can be interpreted as a heavily pruned Volterra series. In fact, it only considers the coefficients that reflect dominant physical hole-electron recombination mechanisms. Evidently, a richer, more generic Volterra model with more degrees of freedom cannot be less effective in addressing the static and dynamic distortion than our solution, as the latter by default forces many coefficients that do not represent a known physical mechanism to zero. Nonetheless, by bounding the room for improvement, we show that the gain to be expected for the generic Volterra solution is negligible and may not justify the added complexity, slower coefficient estimation and the higher power consumption.
- We simulate our algorithms and experimentally verify these with real measurement signals to quantify and benchmark the performance over a range of Signal-to-Noise Ratios (SNRs). That is, measurement results in this work demonstrate that a single-tap second-order non-linear equalizer is able to mitigate the distortion and Inter-symbol Interference (ISI) in LED channels.
- We show that the non-linear equalizer can effectively widen the measured eye diagram of a Pulse Amplitude Modulation (PAM) signal. For DC–offset Optical Orthogonal Frequency Division Multiplexing (DCO-OFDM), our non-linear equalizer can reduce the power consumption by 70% while maintaining constant system throughput. Alternatively, we can improve the system throughput by more than 50% at a constant LED power consumption.

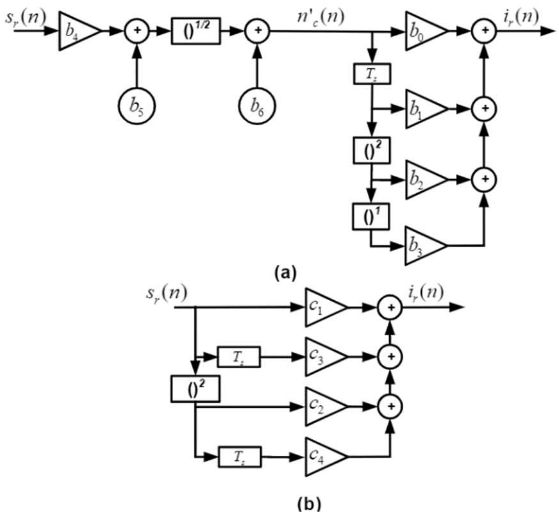

Figure 20: (a) Exact inverse of LED model (post-distorter), (b) The proposed simplified structure.

This project has received funding from the European Union's Horizon 2020 research and innovation programme under grant agreement No 825651 (ELIOT)

We verify that the same structure (Figure 20(b)) can also operate effectively as an equalizer that reduces the MSE, if we appropriately select the parameter setting. We introduce and evaluate an approach that updates the coefficients c_is of the equalizer using MMSE criteria. That is, we use values of incoming signals in our analysis, while the MMSE estimator in the receiver has the task to estimate c_is by correlation of incoming signals with a known training sequence.

This simplified structure reduces the number of independent coefficients from five to three, as elaborated in the Appendix. Since the LED parameters are subject to process spread, to biasing N_c, and may drift over time, these need to be estimated per device and repeatedly. This reduction in model parameters accelerates the acquisition and makes tracking more reliable. Both for PAM and OFDM signals, the simplified equalizer structure substantially improves performance over an approach without equalizer, and is not substantially worse than a more ideal equalization. We simulate and experimentally test over which range of SNR this approach works.

11.1.1 Single-tap second-order non-linear equalizer

One approach, publicly reported by ELiOT in [5], to simplify the square-root operation is a Taylor expansion around the signal mean, which conceptually applies to the concept of DCO-OFDM with a signal probability mass centered near the DC bias. Another approach is a best fit in the range between the LED turn-on current and the maximum signal level used, which conceptually better suits the concept of PAM with equally probable constellation points in the signal range.

11.1.2 Simulation and Practical Verification

We examine the performance of the equalizer structure proposed in Figure 20(b), with the two commonly used signaling methods: PAM and OFDM. The experimental setup is shown in Figure 21(a) with its simplified schematic in Figure 21(b). An Arbitrary Waveform Generator (AWG) created the modulated signal which was converted into current domain by a custom–made LED current driver based on a Minicircuit ZHL-6A amplifier. A bias-T network was used to separately inject the LED DC and AC current components. A resistor was interposed between the amplifier and the Bias-T. The resistor was inserted intentionally not only to protect the power amplifier from being damaged by a mismatching LED load of too low impedance, it also ensures that the amplifier drives the LED with a specific current that is linear with the desired signal waveform. In fact, the resistor ensures that the LED current is not subject to any LED I-V non-linearity. The Bias-T was configured to operate adequately over the entire band, even with an LED dynamic resistance load of less than one Ohm.

A LXML-PB02-0023 blue LED with a measured 3-dB cut-off frequency of 10 MHz at I_{in}= 350 mA bias current was used at the transmitter. At the receiver, we used a Silicon Avalanche Photo-Detector (Si-APD) with 100 MHz 3-dB bandwidth and 1 mm diameter active area followed by a Trans-Impedance Amplifier (TIA). The distance between the LED and the APD was fixed at 1 m. The output signal of the TIA was sampled using a Real Time Oscilloscope (RTO) and delivered to a lab PC for equalization and BER measurement.

This project has received funding from the European Union's Horizon 2020 research and innovation programme under grant agreement No 825651 (ELIOT)

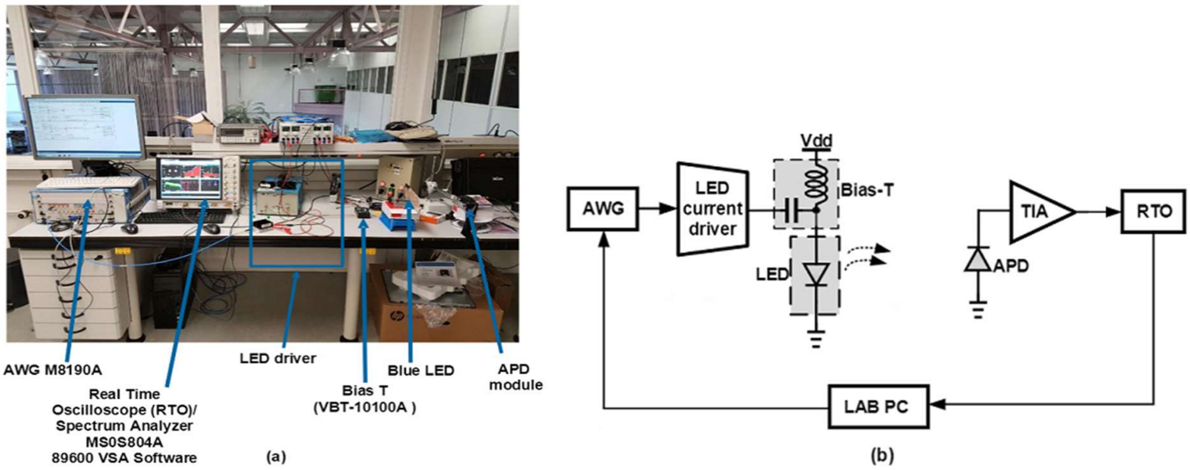

Figure 21: (a) Measurement Setup. (b) Schematic of the setup.

11.1.2.1 Non-linear equalizer in PAM Signalling

For PAM, we numerically simulated to what extent the equalizer improved the Symbol Error Rate (SER) of 4-PAM and 8-PAM. Additionally, using real signals obtained from a hardware setup, we also tested the effect of the equalizer on the eye-diagram of 4-PAM.

We considered three different scenarios. The initial scenario involved no equalization at the receiver. The received noisy signal (after proper scaling) was directly used for SER calculation. In the second scenario, the non-linear terms in the equalizer were forced to zero, hence a first-order MMSE-based linear equalizer was retained. Finally, we tested our non-linear MMSE-based equalizer. The results are given in Figure 22(a) for 20 Msym/sec symbol rate. Due to the non-linear low--pass behaviour of the LED, without any equalization the SER is too large for any practical communication system to handle. Using a linear equalizer can extend the LED bandwidth limitation. However, the BER exceeds the theoretical curve for a flat linear channel at SNRs above 10 dB for 20 Msym/sec symbol rate. This becomes worse at higher rates. For reference, we compare these with an ideal (flat and low-pass) AWGN Linear Time-Invariant (LTI) channel. Using the non-linear equalizer, we reach almost the same performance as in a distortion--free AWGN LTI channel. This observation also indicates that the expected improvement by any other generic and optimized solutions such as Volterra-based compensation is limited and the potential added complexity is not justified. At higher rates, the compensation of the low-pass LED junction inevitably leads to some noise penalty (Figure 22(b)). This is quantified in Figure 22(b), where dotted and dashed lines represent the performance of a fixed MMSE first--order linear equalizer to mitigate ISI in a first--order low--pass LTI channel with 10 MHz bandwidth}. Fig. 42(a), shows that distortion compensation is critical to support 8-PAM.

This project has received funding from the European Union’s Horizon 2020 research and innovation programme under grant agreement No 825651 (ELIOT)

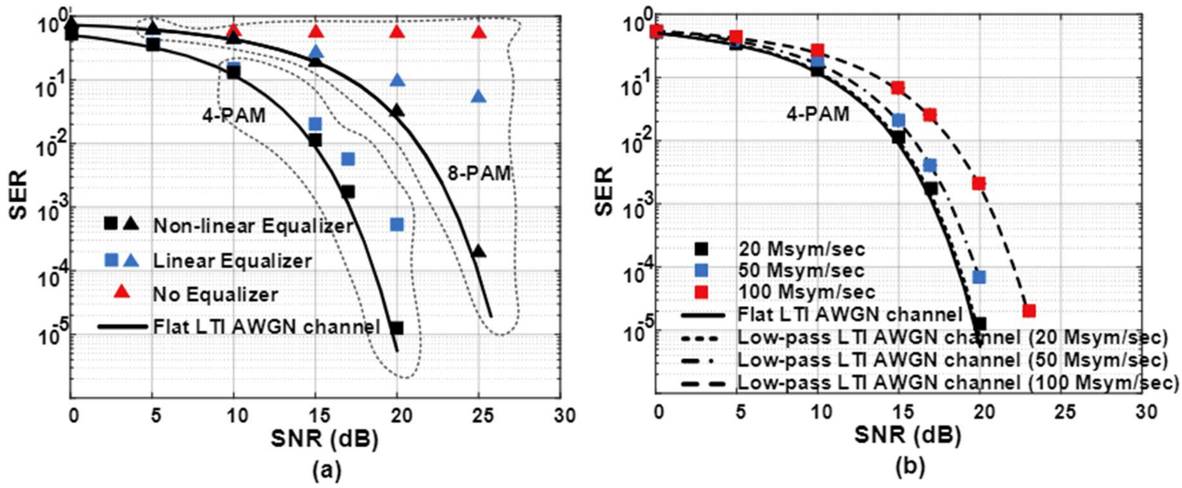

Figure 22: Simulated SER performance for 4-PAM and 8-PAM

Figure 22(a) depicts the simulated SER performance for 4-PAM and 8-PAM signaling at 20 Msym/sec symbol rate. Red triangles (only for 8-PAM) show the SER for the case of no equalization at the receiver. Blue and dark triangles/squares show the SER for having a first–order linear equalizer and for having the proposed non-linear equalizer, respectively. The theoretical limit for uncoded SER for AWGN frequency–flat LTI channel is shown with a solid black line. Figure 22(b) depicts the simulated SER performance of 4-PAM for 20, 50 and 100 Msym/sec using the proposed non-linear equalizer (squares). Bound: SER for distortion-free frequency–flat (solid line) and distortion–free first–order low–pass LTI channel (dotted lines).

To further validate our proposed equalizer structure, the effectiveness of the non-linear equalizer on the eye opening of a 4-PAM signal over optical communication was examined in a real measurement. Fig. 43 shows the eye diagrams of the 4-PAM modulating signal for 5 Msym/s before and after non-linear equalization. It can be seen that the eye diagram of the received 4-PAM signal before non-linear equalization has a right skew, but after applying the non-linear equalization the eye is open and levels are clearly distinguishable.

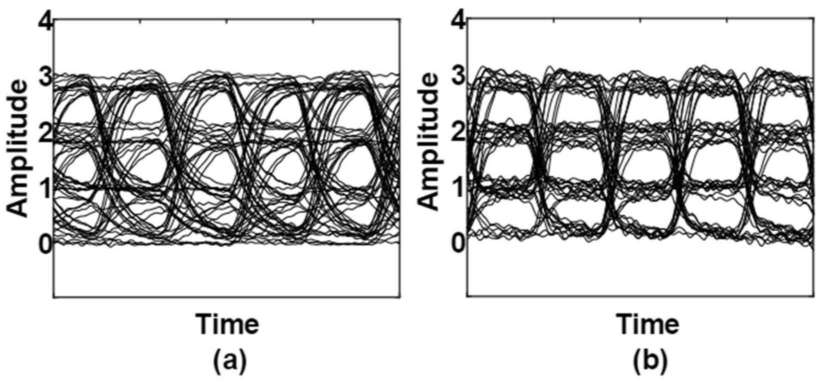

Figure 23: Experimentally measured 4-PAM eye diagrams before (a) and after (b) non-linear equalization

Figure 23 depicts experimentally measured 4-PAM eye diagrams with raised cosine waveform shaping, symbol rate of 5 Msym/s and 30 dB SNR. Where (a) shows the measurements before (with BER = $10^{-2)}$

This project has received funding from the European Union's Horizon 2020 research and innovation programme under grant agreement No 825651 (ELIOT)

and (b) after non-linear equalization. The initial 25 symbols of the PAM signal were used to estimate the equalizer parameters.

11.1.2.2 Non-linear equalizer in OFDM Signaling

In our system, we concatenated our non-linear equalizer, that reduces distortion, with an OFDM system that inherently applies a frequency-domain (linear) equalization. The end-to-end bit loading algorithm optimizes the sub-carrier payload. Figure 24(a) shows the SNR measured at the receiver for two different LED DC currents, 100 mA and 350 mA, with and without enabling the non-linear equalizer. A communication LED, biased at 100 mA with a non-linear equalizer enabled in the receiver, is seen to achieve a better received signal quality than a system without the non-linear equalizer, even if the latter is biased at 350 mA, where more linearity can be expected. That is, the non-linear equalizer saves a significant amount of power (more than 71% reduction in biasing power).

Bringing the bias current back to 350 mA, the non-linear equalizer allows more modulation power and more bits on the sub-carriers: at 40 MHz, the signal-to-noise-plus-distortion is improved by more than 6 dB, allowing the use of 64-QAM modulation, compared to only 8-QAM without the equalizer. The bit-loading profiles with and without running the non-linear equalizer are shown in Figure 24(b), which are limited by detector noise and no longer by distortion. The non-linear equalizer improves the data rate from 303 Mbits/sec to 464 Mbits/sec (more than 53% improvement). Although the non-linear equalizer also compensates the low-pass frequency response, this of course does not improve the signal-to-noise ratio at high frequency as also noise is enhanced. The beneficial effects of the non-linear equalizer are in reducing the distortion, while the OFDM signaling handles the frequency selectivity, after linearization.

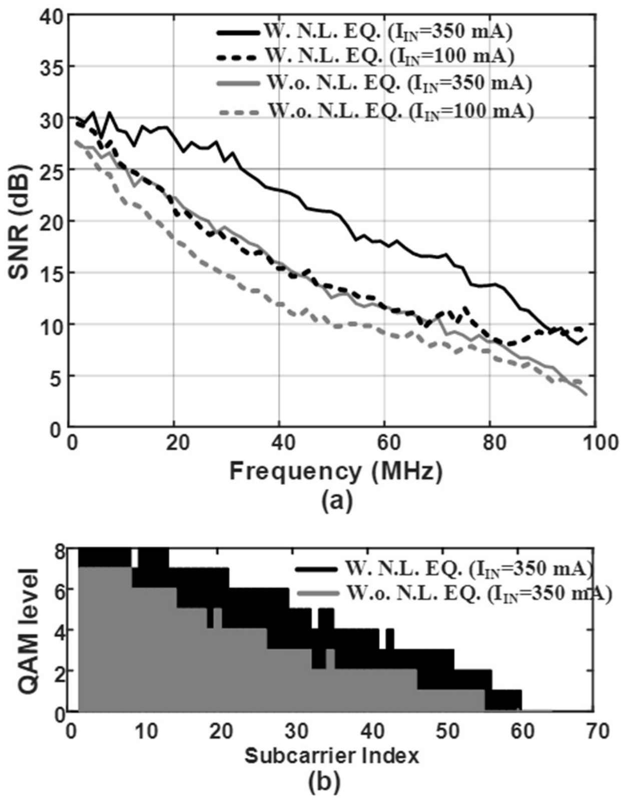

Figure 24: Measured SNR versus frequency

This project has received funding from the European Union’s Horizon 2020 research and innovation programme under grant agreement No 825651 (ELIOT)

Figure 24(a) depicts the measured SNR versus frequency for I_{IN} = 100 mA (dashed) and 350 mA (solid) with (W.) and without (W.o.) non-linear (N.L.) equalizer (EQ.). Figure 24(b) depicts sub-carrier bit loading for I_{IN} = 350 mA to ensure BER $\leqslant 10^{-4}$ with (dark) and without (grey) enabling the non-linear equalizer.

11.2 Conclusions for non-linearity compensation

Mitigation of non-linear distortion is an effective way to reduce power consumption, particularly if high bit rates are desired. The LED is the major source of nonlinearity in a VLC system that limits the achievable bit rate. The recombination rates of photon generation in Double Hetero-structure (DH) LEDs give a mixture of nonlinearities and memory effects. Their mathematical model can be translated into an equivalent discrete-time circuit, that can be inverted. In order to effectively track and compensate for the nonlinearity and memory effects we proposed an MMSE equalizer. This equalizer gives an estimation of the transmitted signal using a single delay tap: sample of the received signal, a previous sample and squares of these are used as four inputs to our design.

The equalization requires to be updated regularly because of variations in LED nonlinearity with time, temperature and different operating regimes, biases, and so on. The alternative of a blind Volterra equalization is computationally complex and time consuming in practical systems. This work has shown that the MMSE equalizer with a single tap of memory and second–order nonlinearity can mitigate the LED distortion efficiently.

The performance of the non-linear equalizer technique was tested in a DCO-OFDM system with an adaptive bit and power loading algorithm. For a required Bit Error Rate (BER), more than 50% higher data rate was achieved for the same power consumption. We expect that on less noisy channels, the gains can be higher. We also saw that the non-linear equalizer can be used to substantially reduce biasing power.

This project has received funding from the European Union's Horizon 2020 research and innovation programme under grant agreement No 825651 (ELIOT)

12 MIMO schemes

Multiple Input Multiple Output was introduced in the field of radio communications and is a set of techniques that enable parallel transmission of data through multiple transmitters and multiple receivers in the same frequency band. It is now routinely deployed in RF systems. In the field of OWC, MIMO has shown its importance as a tool to combat signal blockage and for mobility [61, 62]. So distributed MIMO is an essential ingredient to let LiFi deliver of the promise of providing reliable communication.

We also see MIMO as a means to reduce power, as addressed here in this document. MIMO acts as a gap filler to ensure adequate throughput in areas where a coverage transition occurs from one OFE to another. MIMO allows us to do that with less emitted power, and less waste of power outside what would otherwise be a hard cell boundary where a handover would take place.

Secondly, power considerations in distributed MIMO with LEDs differ from co-located MIMO as commonly used in WiFi. This section addresses how the MIMO operations can adhere to a power limitation per OFE, thus per LED. This is in contrast to a total power, summed over all antenna's as required by radio regulations.

As presented in previous chapters, OFDM is an attractive modulation scheme, sometimes also used to modulate beyond the LED 3-dB bandwidth [8], as it allows for bit and power loading strategies which can explore the frequency roll-off of the devices to improve performance. The combination of OFDM and MIMO combines many advantages from both technologies. When combined, LiFi developers are able to design optimization algorithms to joint optimize the available modulation power among spatial eigenmodes and modulation subcarriers to maximize data rate.

While the MIMO principle has already been explained in previous deliverables, i.e. deliverables 3.4 and 4.2, in this chapter we return to the topic to discuss the power-related optimization problem of maximizing the achievable rate of LED-based D-MIMO OWC systems in different scenarios respecting the power restrictions of the light emitters. It is shown that, in comparison with the uniform spreading of power over the entire bandwidth, the maximization of the achievable rate under a per-LED power constraint achieves better performance and, in some scenarios, also leads to power saving.

12.1 Per LED MIMO optimization

For throughput improvement, many power loading strategies can be used for a total power constraint while allowing power to be freely exchanged among LEDs. In scenarios with unequal distances between LEDs and the user terminal, more power is allocated to the LED that has a stronger channel than to others. However, in practical implementations, each LED is equipped with its own power amplifier and then it is limited individually by the linearity of the amplifier. Besides, the forward drive current of LED should be smaller than a maximum allowable value to ensure that the LED chip does not overheat. Thus, in practice, the MIMO OWC power loading problem should consider a per-LED power constraint, and not just the total average power constraint. This poses new challenges to the design of resource allocation strategies.

This project has received funding from the European Union's Horizon 2020 research and innovation programme under grant agreement No 825651 (ELIOT)

Eliot reported results in [63], that studies to what extent this has an impact on the performance of LED-based distributed MIMO (D-MIMO) OWC links. In [63], the achievable rate optimization problems are formulated for both cases, when the total power is constrained or when under a per-LED power constraint. Results show that, the achievable rate under a per-LED power constraint is lower than under a total power constraint, but it is higher than if the power is uniformly spread over the entire bandwidth. It also allows for transmit power saving, at a cost of higher computational complexity. In addition, it is also shown that under a per-LED power constraint LEDs with better channel condition tends to use a modulation bandwidth far above the 3-dB bandwidth.

As an example Figure 25 gives two scenarios. In the simulations presented here, we considered $N_{sc} = 256$ OFDM subcarriers and the system perform DCO-OFDM. Additional simulation parameters are found in [63].

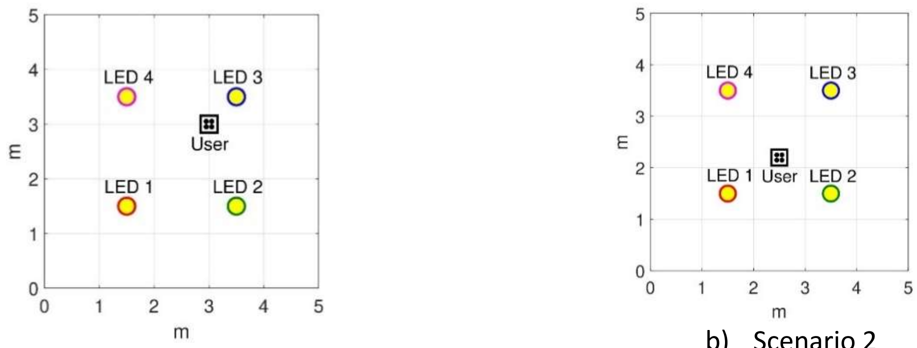

a) Scenario 1

b) Scenario 2

Figure 25: LEDs and user location in scenarios 1 and 2.

Figure 25 a) depicts a first scenario, with a user placed close to one of the LEDs. As the low-pass effect is equal for all LEDs, the difference between values of the LOS channel coefficients strongly depend on the DC-gain, which, in turn, is proportional to the square of the propagation distance. Therefore, for this case, the strongest channel comes from the LED number 3. Figure 25 b) illustrates a second scenario, in which the user is equally distant to LEDs 1 and 2, and also equally distant to LEDs 3 and 4.

Figure 26 shows the achievable rate for each one of the three different power loading strategies in both considered scenarios. As can be observed, the unrealistic approach that allows the exchange of energy between LEDs has achieved highest performance in both scenarios. As expected, the uniform power loading scheme achieved the lowest performance due to its inability to adapt the power distribution over the low-pass channel. Moreover, the maximization of the achievable rate under a per-LED power constraint achieved higher performance than uniform loading in both scenarios. If LEDs are at approximately equal distances from the user, as in scenario 2, the total-power constraint already balances power well over all LEDs. So, per-LED and total-power constraints perform more equal in scenario 2 than in scenario 1.

This project has received funding from the European Union's Horizon 2020 research and innovation programme under grant agreement No 825651 (ELIOT)

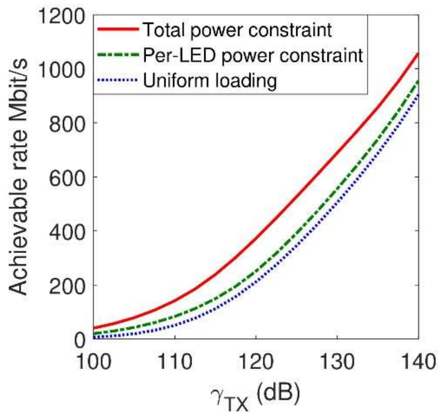

a) Achievable rate: scenario 1

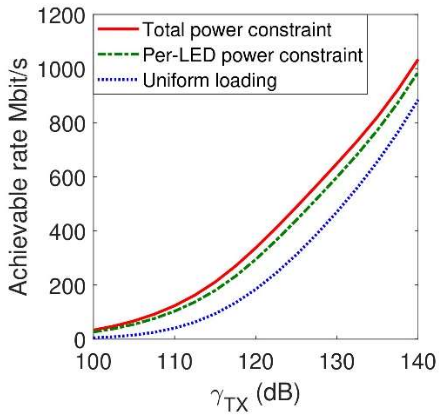

b) Achievable rate: scenario 2

Figure 26: Achievable rate of a 4×4 LED-based D-MIMO OWC system in scenarios 1 (a) and 2 (b).

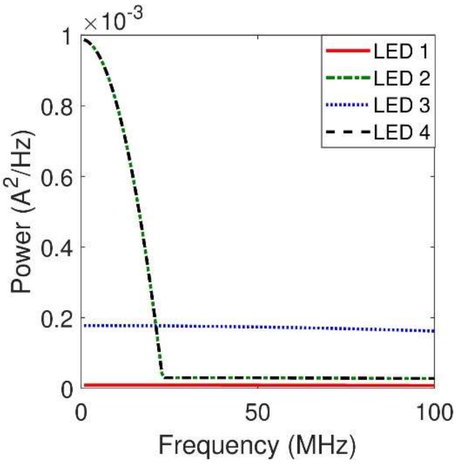

a) Per-LED power constraint: scenario 1

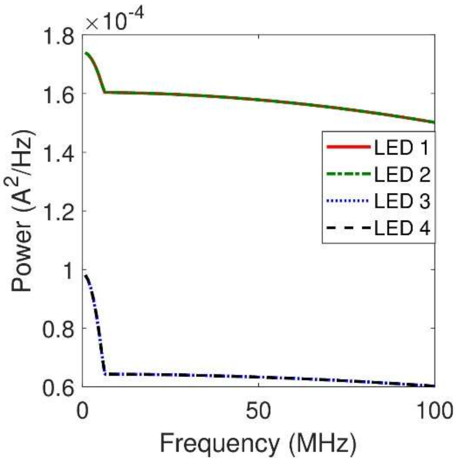

b) Per-LED power constraint: scenario 2

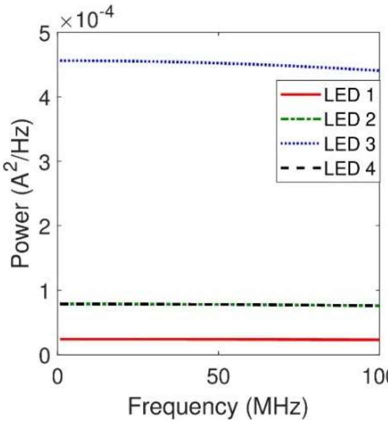

c) Total power constraint: Scenario 1

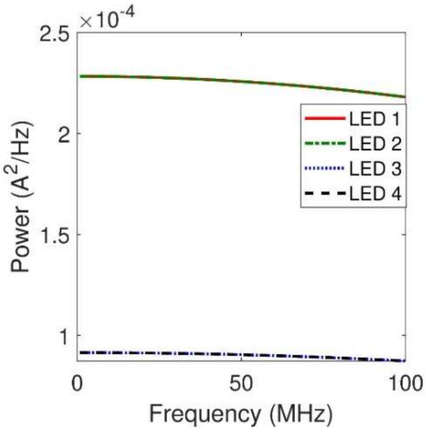

d) Total power constraint: 2

Figure 27: Power distribution on each LED over the modulation frequency band. For scenario 1: (a) and (c). For scenario 2: (b) and (d). $\gamma_{TX} = 130$ dB.

This project has received funding from the European Union's Horizon 2020 research and innovation programme under grant agreement No 825651 (ELIOT)

To further explore the problem, Figure 27 shows the power distribution over the LEDs for each one of the power loading strategies. As known from water-filling solutions, the best strategy to achieve high throughput is to allocate more power on the strongest channels. Then, as anticipated, both power loading strategies under total and per-LED power constraints seek to allocate more power on the LEDs close to the user.

However, in contrast to Figure 27 b) and Figure 27 d) , Figure 27 a) and Figure 27 c) shows the power distribution computed by maximization under the per-LED power constraint. It ensures that not more power will be allocated to one LED than its maximum supported value. Thus, instead of allocating almost all power, e.g. $\approx 2.8\sigma_{max}^2$ to LED 3 only by the total-power constraining approach in the first scenario, the per-LED power loading strategy is forced to allocate power to the neighboring LEDs. In scenario 1, almost no power is allocated in LED number 1, for a total as well as for a per-LED power constraint. A total power constraint has little impact since this amount of power is relocated to other LEDs closer to the user. However, the approach constrained by the per-LED constraint leads to a power-saving since part of the available total power remains unused. Nonetheless, the achievable rate is still higher than the uniform loading strategy even with less power allocated to one of the LEDs. It yields a power reduction of almost 24% of the power consumed by modulation in the first scenario.

Figure 27 further confirms that, in order to achieve high throughput, also MIMO optimization algorithms favor strong channels for a modulation bandwidth that is far above the LED 3-dB bandwidth, as seen in [8] for single-input single-output (SISO) systems.

12.2 ELIoT conclusion for MIMO constraints

The obtained results bring interesting conclusions such as: In some scenarios, a per-LED power constraint substantially reduces the achievable throughout compared to a total power constraint that allow exchange of a power budget of one LED to another. Spread uniformly the total average modulation power over the entire modulation bandwidth of the LEDs is not efficient due to its low-pass effect. Due to the LED characteristics, a user close to an LED may be able to use a large modulation bandwidth of this LED while a just small portion of the modulation bandwidth of the others is used, or they are almost not used. The simulations also show that, the approach which allows power exchange among LEDs is undesirable as it tends to allocate more power to the nearest LED than the device is capable of supporting. If all LEDs see more or less equal attenuation to the client device, the differences vanish.

In summary, ELIoT presented a detailed model to estimate the achievable rate of an LED-based D-MIMO OWC system under two different power constraints. These are a total power constraint, in which LEDs are allowed to exchange power between them, and a per-LED power constraint, in which the amount of power consumed by each individual LED is limited. Based on these two power constraints, three different power loading strategies have been addressed. These are uniform power over the entire bandwidth, maximization of the achievable rate under a total power constraint, and maximization of the achievable rate under a per-LED power constraint. It was shown that the maximization of the achievable rate under a per-LED power constraint is more appropriate for real systems. In addition, it has the advantage of a better performance than a uniform power loading strategy and it allows power saving. However, its computational complexity is larger.

This project has received funding from the European Union's Horizon 2020 research and innovation programme under grant agreement No 825651 (ELIOT)

13 Unipolar OFDM

A further measure to reduce the power consumption of optical OFDM is to avoid the use of a DC bias. A large variety of solutions have been proposed to make the OFDM signal non-negative, to fit the Intensity Modulation of light [64]. ACO-OFDM [65, 66, 67, 68] and Flip-OFDM [69, 13] appear to be basic concepts which is elaborated upon. Hitherto, these two systems have been compared by simulation. Yet, an inherent similarity in the mathematical formulation of ACO-OFDM and flip-OFDM allows a harmonization into a common description, which can facilitate standardization and help to build an intuition for further improvements. It can also help to understand performance observations made in previous simulations. Moreover, based on these insights novel implementations are possibly for a broad class of unipolar and hybrid OFDM schemes.

An elaborate, more mathematically-heavy version of this text is in our paper [13]. Our analysis explains why so many simulations have shown similar performance of ACO and flip OFDM. In our paper [13], we further show that although ACO OFDM gains in power efficiency over DCO-OFDM because it does not need a bias, there is a 3 dB penalty to ACO-OFDM and Flip OFDM as it (un-flips and) merges two OFDM blocks while each signal sample only is present in either the first or in the second block, while noise is present in both blocks. This effect reduces the BER by 3 dB. Another way of explaining this is a by saying that the clipping operation smears 50% of the signal power outside the subcarrier spectrum that is seen by the receive FFT. This 3 dB loss consumes a substantial amount of the power-efficiency gains that are attributed to ACO OFDM.

13.1 ELIoT conclusions on Unipolar OFDM

Both Flip-OFDM and ACO-OFDM start by creating an OFDM signal in which the second half is exactly a polarity-flipped replica of the first part. Flip OFDM does this by repeating and polarity-flipping a OFDM block of length N. ACO-OFDM does this by using an FFT of length $2N$ and only allowing signal dimensions that have the required period repetition, i.e., the odd subcarriers.

An advantage of ACO OFDM is that all (odd) subcarriers are by design continuous at the split between the two halves. So, the cyclic prefix and windowing are only needed at the beginning of the $2N$ frame, while Flip OFDM would need cyclic prefixes and windowing at both halves.

ACO-OFDM is very similar to Flip-OFDM, except that all subcarriers are shifted one frequency grid-point upwards. It appears that by shifting up all subcarriers have a continuous phase halfway the frame, one can spectrally contain the signal better.

We can propose a subtle modification to FLIP OFDM that yields these two advantages: Continuous Phase Flip-OFDM. The idea is to multiply the entire sequence by a complex exponential, that mimics a frequency lift of half a subcarrier.

The Hermitian symmetry of the OFDM input signal does not need to be created explicitly. It suffices to only feed the FFT with complex QAM data for the first half of all subcarriers and leave the rest as zeros. At the output of the FFT one can the take the real part of the signal.

This project has received funding from the European Union's Horizon 2020 research and innovation programme under grant agreement No 825651 (ELIOT)

There appears to be a new versatile signal processing recipe that can create both Flip-OFDM and ACO-OFDM. It uses only an *N*-sized FFT, it copies the first halve into a second block and clips the lower half. A new ACO-OFDM modulator and receiver can consist of an FFT only of size N, but merges two halves before FFT.

ACO-OFDM and Flip-OFDM gain in power-efficiency as these do not require a DC bias while DCO-OFDM does require a bias. Yet, a 3 dB loss is incurred if an FFT is used to receive these unipolar schemes via an FFT OFDM receiver.

This project has received funding from the European Union's Horizon 2020 research and innovation programme under grant agreement No 825651 (ELIOT)

14 ELIOT Suggestions and Recommendations for ITU g.hn

This section lists some ideas to optimized LiFi standards and systems, in particular to improve power consumption and to reduce overhead. The section shows that the bit loading scheme can be further optimized for the LED communication. The LED channel is characterized by a transfer function that is predominantly declining with frequency.

In particular, an algorithm is described that allows the exchange of a SNR margin on some subcarriers, to improve the SNR on subcarriers that experiences poorer channel responses. It combines a number of subcarriers to obtain more equally distributed SNRs. Subcarriers with an excess margin in SNR are used to help subcarriers with insufficient SNR.

This low-pass nature of LEDs, in particular, its junction capacitance and delaying time constants in hole electron recombination, deteriorates major portions of the spectrum while these can still contribute to the throughput. OFDM allows the use of different parts of the spectrum with a specific power and signal constellation. In more heavily attenuated parts of the spectrum, larger or lower powers can be used (i.e., power loading), and signals at higher-attenuated frequencies, which contain a relative larger amount of noise, more robust signals can be used. That is, smaller constellations that carry fewer bits can be used at higher frequencies (i.e., bit loading).

Contributions towards a more effective use of the link-budget, thus allowing a lower power consumption or enabling a higher bit rate, include

- Adaptive choice of bandwidth, using a bandwidth optimized for the given link budget. We use insights from [8].
- Exchange of SNR: a SNR-trading approach that combines a number of subcarriers to get more equally distributed SNRs. Subcarriers with a margin in SNR are used to help subcarrier with insufficient SNR.
- Efficient data format to identify the chosen modulation per subcarrier

14.1 Format for signalling bit loading profile

It is very inefficient to describe separately which constellation is used for every subcarrier. As systems typically use 512, 1024 or even 2048 or more subcarriers, it may require excessively many parameters to be exchanged. This may have been one of the reasons that historically prohibited the use of adaptive bit loading in radio frequency (RF) systems. In RF radio systems, adaptive bit loading is less a necessity, because typical fades experienced in RF communications are not very wide, thus only affect a few subcarriers. Error correction, particularly in combination with bit interleaving adequately solves the problem of fades in most RF systems.

However, for OWC the typical transfer functions have wide bandwidths of deep attenuation. These can be caused by a decline of responsivity of the LED at high modulation frequencies. Another cause of wide fades can be multipath reception with a short delay spread, as for instance seen in indoor communication in which the direct path and the reflected path only have a minor length difference. Thirdly, if multiple light sources carry the same data, but are connected via cables of slightly different

This project has received funding from the European Union's Horizon 2020 research and innovation programme under grant agreement No 825651 (ELIOT)

length, say a few meters differences, a wide null may occur at modulation frequencies of a few tens of MHz.

The corresponding distortions can cause a problem in LiFi using LEDs, as wide fades cannot easily be resolved by error correction coding, because too many subcarriers may be lost to recover the signal. Adaptive bit loading, in which these poorly performing subcarriers, i.e., those in a fade, are skipped or modulated by only a small number of bits, thus a more robust constellation, is important.

But one can exploit the observation that the LED channel mostly is a monotonously declining function, and that many neighbouring subcarriers have the same constellation. This may not be the case if multipath reflections occur in the wireless channel or if a fade created by two spatially separated TX's send the same signal. This may be resolved by maintaining an option to fall back to existing signalling methods that do not exploit monotonicity. Nonetheless, we have seen the monotonous character in most practical situations.

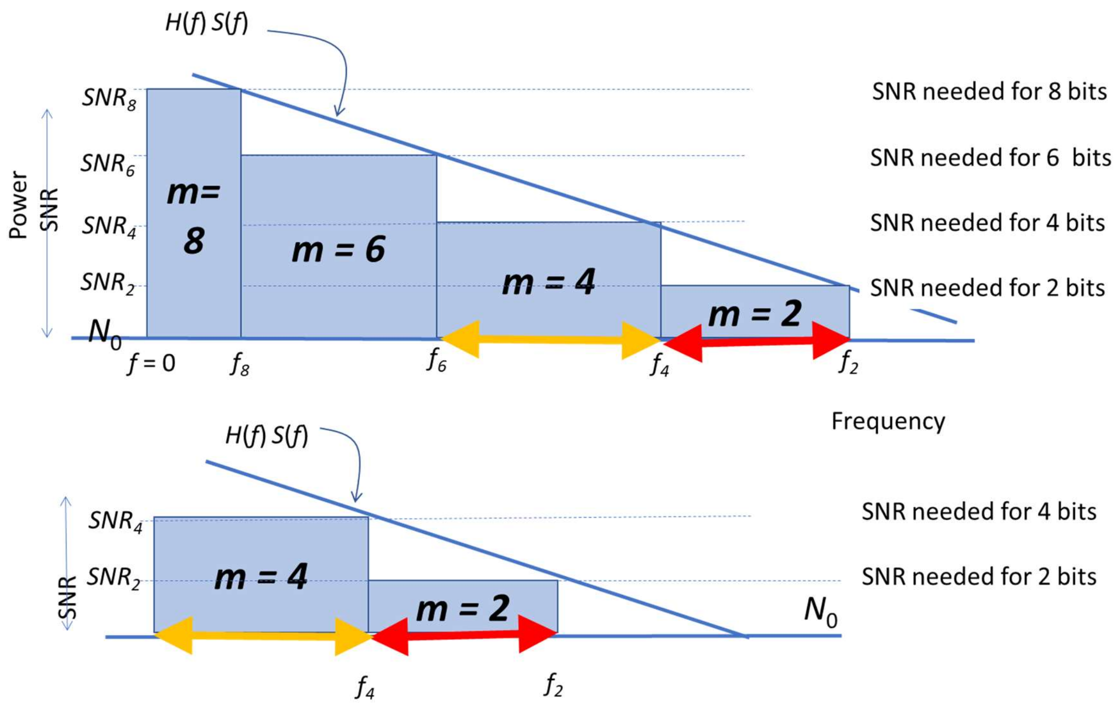

Figure 28: Influence of number of OFDM subcarriers

Figure 28 illustrates that regardless of the SNR, for a typical LED profile, the number of subcarriers that can carry 2 bits is a system constant (red arrow bandwidth). Similarly, a constant number of subcarriers can carry 4 bits (orange arrow bandwidth).

So, we conclude that the "profile" of how many subcarriers can carry "X" bits can be exchanged once. During operation, the system only needs to shift this profile left or right (and only use positive subcarriers, or subcarriers above a minimum frequency) In other words, instead shifting the profile in vertical direction (more (less) bit on each subcarrier), one may shift sidewards, and use the same bit loading profile, but shifted in frequency.

This project has received funding from the European Union's Horizon 2020 research and innovation programme under grant agreement No 825651 (ELIOT)

14.2 Efficient Data Format for how subcarriers are loaded

It is inefficient in terms of communication signalling overhead, for every subcarrier to describe which constellation is used. We exploit the fact that the LiFi channel is a monotonously declining function, and that many neighbouring subcarriers have the same constellation.

In order to simplify the overhead in signalling what constellations are used, ITU G.9991 already uses a grouping of neighbouring subcarriers, that all have the same constellation. Then, a single identifier can be used to communicate the constellation for all subcarriers that are part of the group. Yet, further identifiers are needed to describe which subcarriers belong to the group. Here, one can exploit the monotonously declining frequency response of the LED.

ITU G.9991 already describes "grouping" of neighbouring subcarriers that use the same constellation. During an initial phase of the system, a channel estimation process is launched and the constellations to be used in each of the groups is calculated by the receiver node BAT (bit allocation table) and sent to the transmitter node with a particular identifier. The transmitter node uses this BAT when creating its transmission signal. Since the identifier is signalled in the header of each transmission, the receiver node knows which constellation to use for each subcarrier. After this initial phase, the receiver keeps track of the channel characteristics by estimating over the data frames. Minor changes trigger a partial update procedure, where part of the BAT is updated and sent to the transmitter. If a substantial change in the channel occurs, a new channel estimation is triggered.

A full channel estimation process is quite costly in terms of overhead since it involves the exchange of several frames with many bits of information per subcarrier and involves significant periods of throughput decrease.

This process does not exploit the property that on an LED channel, constellation sizes mostly monotonously decrease. In particular, for an LED response that declines exponentially with frequency, which approximates well many measured LED channels [8]. If we also consider gentle multipath and PD capacitances at the detector, further monotonically declining effects are added.

14.3 Adaptive bandwidth

As shown above, using a fixed bandwidth is not optimum for a power-limited (rather than a PSD limited) link. As a first step, high subcarriers not used for communication, should be switched off. Secondly, the power gained by switching off these subcarriers can be re-applied at lower frequencies. As a simplified implementation, the communication bandwidth can be halved and a gain of 3 dB can be applied during conditions of a poor signal-to-noise ratio. As an example, in G.9991 Coax mode, a bandwidth of 100 MHz can be reduced to 50 MHz. Yet better is a fully adaptive bandwidth selecting algorithm.

Today this is not possible in G.9991 in a dynamic way since a change of bandwidth needs the negotiation of many parameters, a new channel estimation and the bandwidths to be used are set "per network" and not "per node". However, there is no barrier to implementing this feature since the run-time communication between two nodes necessitates only the exchange of the information of which constellation to be used between a starting frequency and an end frequency. The reason why

This project has received funding from the European Union's Horizon 2020 research and innovation programme under grant agreement No 825651 (ELIOT)

this is not practically implemented in the standard is that a dynamic exchange of such information would mean continuous estimations of the channel with disruptions in the throughput and latency. However, several techniques have been introduced in ELIOT project to accelerate this change of information and several BATs can be stored in parallel for different bandwidths and communicated by the transmitter in the header.

14.4 Exchange of SNR

We see that for uniform power loading, the link wastes (1.5 to) 3 dB by only taking an integer number of bits per subcarrier. Here we show that we can recover this loss, thus reduce the power consumption by tens of precents.

In a system with uniform power loading, the power per subcarrier does to exactly match the SNR required for a constellation with an integer number of bits. Some subcarriers have an excess of SNR, that ranges from 0 to (3 or) 6 dB, depending on the set of constellations used in the system. This headroom in SNR is not used to effectively achieve the maximum throughput as no suitable constellation exists or can be used that fully utilizes the available SNR.

For QAM with an even number of bits, thus an integer number of bits per in-phase and quadrature-phase dimension as in 4, 16, 64, 256, 1024 QAM, a 6 dB step size applies, so an average penalty of 3 dB occurs. This loss is significant and substantially reduces the range at which the system can work or doubles the power consumption of the dongle and ceiling infrastructure.

It has been argued, e.g. by [8], that if constellations can be even or odd integer numbers of bits in QAM, thus including non-square constellations, i.e. stepping from 2, 4, 8, 16, 32, 64, 128, 256, 512, 1024, … QAM, this leads to a gap in performance of 1.5 dB (rather than 3 dB). This is still a significant loss, but it can, for instance, be exploited as a 30 percent lower power consumption.

As we will show next, this inefficiency gap can be repaired. We show that the excesses of SNR on some subcarriers can be exchanged with other subcarriers. This allows subcarriers which have just-too-little SNR to be boosted to reach an adequate SNR. This can be done without changing the power spectral density of the subcarriers, thus without deviating from certain power loading.

It appears possible to exchange an excess in SNR on one frequency to repair a shortage in SNR at another frequency. A special form of multiplexing can be used. In a basic form, one can transmit the sum of two data symbols on one frequency and the difference of the data symbols at another frequency. That is, a simple pre-processing before the transmit i-th FFT is proposed. If the receiver does the inverse, the original symbols are recovered, but the noise level is averaged of the to two data symbols.

These sums and differences can be generalized as a unitary matrix operation over N incoming data symbols, into N outgoing subcarriers. Preferably the matrix just contains +1 (addition) and -1 (subtraction) weight factors and more preferably a Walsh Hadamard matrix is used.

This procedure would not result in a significant change in the channel estimation protocol and would not introduce significant additional overhead. However, the modulation scheme would change

This project has received funding from the European Union's Horizon 2020 research and innovation programme under grant agreement No 825651 (ELIOT)

considerably, meaning that the use of such feature would need to be negotiated before its use and therefore it cannot be switched on and off dynamically.

14.5 ELIoT conclusion for Bit loading

We identified improvements for ITU-T G.9991 that significantly enhance the power efficiency, or that can be used to increase throughput of the system. In contrast to tracking the rapid multipath fading in RF, in OWC the overhead on adaptive bit loading can be contained to a reasonable amount. Thereby one can get the benefits, which are high on OWC LED channels. An exchange of SNR can be used for a LiFi System with a low pass frequency response and specifically exploit excessive SNR on some subcarriers that would otherwise be wasted. While the proposed mechanisms cannot be directly supported by current state of ITU-T G.9991 standard, an early analysis of their inclusion in the channel estimation process of this standard has been realized.

In order to include these new concepts into the ITU-T family of standards, an amendment document to ITU-T G.9991 needs to be prepared. The amendment document can be started at any time by a decision of the standardization group.

A first step towards the inclusion of the different potential improvements identified in the standard for improving the data format, the subcarrier bitloading, the exchange of bitloading and SNT information between nodes and adaptive bandwidth will be to prepare technical contributions to the standard dealing with:

- The technical improvement that the proposal brings, providing technical data coming from the ELIOT project (including simulation results and precise description of the algorithms) on the merits of the proposed solution compared to the current status of the system in the standard.
- Any technical proposal to an existing standard needs to deal with the issue of the “backwards compatibility”. Any proposal has to describe how the new feature will be used in a context where nodes in the network may not implement this new feature and may not even be aware of the existence of this issue. In this sense, a new proposal in an amendment is always optional in the standard and any new node has to signal its capability to use it (normally, through the capability exchange protocol during the registration phase)
- Finally, a preliminary proposal on the changes that are needed in the standard to accommodate the new feature. This is generally done by proposing draft text to be incorporated to the standard

While the first issue has been covered in their majority by the technical work done in ELIOT, the other two need further work.

These three points are normally handled sequentially with individual contributions by members of ITU-T (in this case, several partners in ELIOT are members of ITU-T and therefore can convey ELIOT results into the standardization process). Once a proposal (first bullet) is presented in the relevant ITU-T group, a technical discussion is started with all the involved parties providing comments, suggestions and criticism. After the group reaches an agreement (consensus) on the interest of including this new feature (normally, with additions from other parties), the group decides on how to

This project has received funding from the European Union’s Horizon 2020 research and innovation programme under grant agreement No 825651 (ELIOT)

handle backwards compatibility. Finally, the draft text is written by the interested parties and adopted as draft by the group.

The above-described process takes roughly 6 to 9 months to be completed. This means that from an ELIOT project perspective, a first draft with the proposed changes could be completed by the end of 2022.

Once the draft text is ready, the group will proceed to "consent" the changes at an ITU-T SG15 plenary and open a comment period where any interested party member of the ITU-T can provide proposals for improvements on the new additions. It is expected that members of ELIOT that worked on the proposal will participate in this "Last Call" comment resolution process during the first half of 2023.

Once all the comments have been addressed by the group, a new phase ("Additional Review") will start and if no comments are received (which is the normal case), the new amendment to G.9991 will be approved (mid of 2023) and published by ITU-T.

Following this process, it is expected that the new proposed mechanisms for allowing a rapid track of the changes in the LiFi channel can be officially incorporated in the standard by middle of 2023.

The LED channel gives quite severe attenuation at higher frequencies. That differs from a typical radio (Rician) multipath channel. We show that for the LED channel, uniform power loading can improve its link budget by 1.5 to 3 dB by using the SNR trade and exchange approach.

This project has received funding from the European Union's Horizon 2020 research and innovation programme under grant agreement No 825651 (ELIOT)

15 Concluding Remark

In this document, we summarised a number of opportunities to reduce the power of LiFi systems. Some of these can be implemented in systems that use existing ICs. Other concepts require a deeper modification of the firmware and the silicon. All in all, the ELIoT consortium believes that there is a viable path forward to make LiFi a competitive, energy efficient option for wireless communication

This project has received funding from the European Union's Horizon 2020 research and innovation programme under grant agreement No 825651 (ELIOT)

16 References

[1] A. Alexeev, J.-P. M. G. Linnartz, K. Arulandu and X. Deng, "Characterization of dynamic distortion in LED light output for optical wireless communications," *Photonics Research,* vol. 9, no. 6, pp. 916-928, 2021.

[2] X. Deng , S. Mardanikorani, Y. Wu, K. Arulandu, B. Chen, A. M. Khalid and J.-P. M. G. Linnartz, "Mitigating LED Nonlinearity to Enhance Visible Light Communications," *IEEE Transactions on Communications,* vol. 66, no. 11, pp. 5593 - 5607, 2018.

[3] J.-P. Linnartz , "A New LED Communication Model Based on Photonic Properties," in *PIMRC2021*, Online, 2021.

[4] J.-P. M. G. Linnartz, X. Deng and P. Van Voorthuisen, "Impact of Dynamic LED Non-Linearity on DCO-OFDM Optical Wireless Communication," *IEEE Communications Letters,* vol. 25, no. 10, pp. 3335 - 3339, 2021.

[5] S. Mardani, A. Alexeev and J.-P. Linnartz, "Modeling and compensating dynamic nonlinearities in LED photon-emission rates to enhance OWC," in *SPIE OPTO*, San Francisco, California, United States, 2019.

[6] J.-P. M. Linnartz and X. Deng, "Progressing insights in signal processing for optical wireless communications," in *Symposium on Information Theory and Signal Processing in the Benelux*, TU Eindhoven, 2021.

[7] S. Mardanikorani , X. Deng and J.-P. M. G. Linnartz, "Optimization and Comparison of M-PAM and Optical OFDM Modulation for Optical Wireless Communication," *IEEE Open Journal of the Communications Society,* vol. 1, pp. 1721 - 1737, 2020.

[8] S. Mardanikorani, X. Deng and J. M. G. Linnartz, "Sub-Carrier Loading Strategies for DCO-OFDM LED Communication," *IEEE Transactions on Communications,* vol. 68, no. 2, pp. 1101-1117, 2020.

[9] X. Deng , K. Arulandu, Y. Wu, S. Mardanikorani, G. Zhou and J.-P. M. G. Linnartz , "Modeling and Analysis of Transmitter Performance in Visible Light Communications," *IEEE Transactions on Vehicular Technology* , vol. 68, no. 3, pp. 2316 - 2331, 2019.

[10] K. Arulandu, J. -P. M. G. Linnartz and X. Deng, "Enhanced Visible Light Communication Modulator With Dual-Feedback Control," *IEEE Journal of Emerging and Selected Topics in Power Electronics,* vol. 9, no. 1, pp. 123-137, 2021.

[11] J.-P. Linnartz, P. v. Voorthuisen and C. Hoelen, "Enhancing Indoor Optical Wireless Communication System Performance by Sectorization," in *Proc. SPIE*, 2022.

This project has received funding from the European Union's Horizon 2020 research and innovation programme under grant agreement No 825651 (ELIOT)

[12] J.-P. Linnartz, C. Hoelen, P. v. Voorthuisen, T. E. B. Cunha and H. Tao, “LED assessment based on an improved quality factor for LiFi communication,” in *Proc. SPIE*, 2022.

[13] J.-P. M. Linnartz and X. Deng, “Continuous phase Flip-OFDM in optical wireless communications,” *Signal Processing,* vol. 182, p. 107963, 2021.

[14] Hinrichs, M. et al., “Demonstration of Optical Wireless COmmunications Using the Pulse Modulation PHY in IEEE 802.15.13,” in *2020 22nd International Conference on Transparent Optical Networks (ICTON)*, 2020.

[15] D. J. F. Barros, S. K. Wilson and J. M. Kahn, “Comparison of Orthogonal Frequency-Division Multiplexing and Pulse-Amplitude Modulation in Indoor Optical Wireless Links,” *IEEE Transactions on Communications,* vol. 60, no. 1, pp. 153-163, 2012.

[16] J. Lian, M. Noshad and M. Brandt-Pearce, “Comparison of Optical OFDM and M-PAM for LED-Based Communication Systems,” *IEEE Communications Letters,* vol. 23, no. 3, pp. 430-433, 2019.

[17] A. Nuwanpriya, S. -W. Ho, J. A. Zhang, A. J. Grant and L. Luo, “PAM-SCFDE for Optical Wireless Communications,” *Journal of Lightwave Technology,* vol. 33, no. 14, pp. 2938-2949, 2015.

[18] X. Ling, J. Wang, X. Liang , Z. Ding and C. Zhao, “Offset and Power Optimization for DCO-OFDM in Visible Light Communication Systems,” *IEEE Transactions on Signal Processing,* vol. 64, no. 2, pp. 349 - 363, 2015.

[19] S. Dimitrov and H. Haas, “Information Rate of OFDM-Based Optical Wireless Communication Systems With Nonlinear Distortion,” *Journal of Lightwave Technology,* vol. 31, no. 6, pp. 918-929, 2013.

[20] R. G. Gallager, Information Theory and Reliable Communication, New York, NY, USA: Wiley, 1968.

[21] D. Hughes-Hartogs, “Ensemble modem structure for imperfect transmission”. U.S. Patent 4 679 227, 1987.

[22] D. Hughes-Hartogs, The capacity of a degraded spectral Gaussian broadcast channel, Stanford, CA, USA: Ph.D. dissertation, Inf. Syst. Lab., Center Syst., 1995.

[23] J. A. C. Bingham, “Multicarrier modulation for data transmission: an idea whose time has come,” *IEEE Communications Magazine,* vol. 28, no. 5, pp. 5-14, 1990.

[24] B. Cardiff, M. F. Flanagan, F. Smyth, L. P. Barry and A. D. Fagan, “On Bit and Power Loading for OFDM Over SI-POF,” *Journal of Lightwave Technology,* vol. 29, no. 10, pp. 1547-1554, 2011.

[25] L. Goldfeld, V. Lyandres and D. Wulich, “Minimum BER power loading for OFDM in fading channel,” *IEEE Transactions on Communications,* vol. 50, no. 11, pp. 1729-1733, 2002.

This project has received funding from the European Union’s Horizon 2020 research and innovation programme under grant agreement No 825651 (ELIOT)

[26] "ITU-T Study Group 15, Recommendation ITU-T G.9991 High speed indoor visible light communication transceiver – System architecture, physical layer and data link layer specification, 2019".

[27] "Status of IEEE 802.11 Light Communication TG," [Online]. Available: http://www.ieee802.org/11/Reports/tgbbupdate. [Accessed Jul. 2020].

[28] H. Le Minh, D. O'Brien, G. Faulkner, L. Zeng, K. Lee, D. Jung, Y. Oh and E. T. Won, "100-Mb/s NRZ Visible Light Communications Using a Postequalized White LED," *IEEE Photonics Technology Letters,* vol. 21, no. 15, pp. 1063-1065,, 2009.

[29] C. Chen, D. A. Basnayaka and H. Haas, "Downlink Performance of Optical Attocell Networks," *Journal of Lightwave Technology,* vol. 34, no. 1, pp. 137-156, 2016.

[30] J.-P. M. G. Linnartz, X. Deng, A. Alexeev and S. Mardanikorani, "Wireless Communication over an LED Channel," *IEEE Communications Magazine,* vol. 58, no. 12, pp. 77 - 82, 2021.

[31] Hinrichs, M. et al., "Pulsed Modulation PHY for Power Efficient Optical Wireless Communication," in *IEEE International Conference on Communications (ICC)*, 2019.

[32] I. 8. W. T. G. 13, "Multi-Gigabit/s Optical Wireless Communications," 2018. [Online]. Available: http://www.ieee802.org/15/pub/TG13.html.

[33] "ITU-T Study Group 15, Recommendation ITU-T G.9960 Unified high-speed wireline-based home networking transceivers (G.hn) – System architecture and physical layer specification, 2018".

[34] M. Hinrichs, B. Poddig, M. Nölle, P. Hellwig, R. Freund and V. Jungnickel, "Efficient Line Coding for Low-Power Optical Wireless Communication," *VTC2021-Fall Workshop on Optical Wireless Communication (OWC)],* 2020.

[35] J. Armstrong, "OFDM for Optical Communications," *Journal of Lightwave Technology,* vol. 27, no. 3, pp. 189-204, 2009.

[36] S. Mardanikorani and J. M. Linnartz, "Capacity of the first-order low-pass channel with power constraint," in *Symposium on Information Theory and Signal Processing in the Benelux*, Enschede, The Netherlands, 2018.

[37] S. Mardanikorani, X. Deng and J.-P. M. G. Linnartz, "Sub-Carrier Loading Strategies for DCO-OFDM LED Communication," *IEEE Transactions on Communications,* vol. 68, no. 2, pp. 1101 - 1117, 2019.

[38] D. Schneider, . A. Shrotri, H. Flatt, O. Stübbe and R. Lachmayer, "Efficient visible light communication drivers using illumination LEDs in industrial environments," in *SPIE Optics + Optoelectronics*, Online Only, 2021.

This project has received funding from the European Union's Horizon 2020 research and innovation programme under grant agreement No 825651 (ELIOT)

[39] J. J. D. McKendry, D. Massoubre, S. Zhang, B. R. Rae, R. P. Green, E. Gu, R. K. Henderson, A. E. Kelly and M. D. Dawson, “Visible-Light Communications Using a CMOS-Controlled Micro-Light-Emitting-Diode Array,” *Journal of Lightwave Technology,* vol. 30, no. 1, pp. 61 - 67, 2011.

[40] H. Fu and Y. Zhao, “Nitride Semiconductor Light-Emitting Diodes (LEDs) (Second Edition),” in *9 - Efficiency droop in GaInN/GaN LEDs*, Woodhead Publishing, 2018, pp. 299-325.

[41] E. Kioupakis, Q. Yan, D. Steiauf and C. G. Van de Walle, “Temperature and carrier-density dependence of Auger and radiative recombination in nitride optoelectronic devices,” *New Journal of Physics,* vol. 15, no. 12, p. 125006, 2013.

[42] H. Chun, S. Rajbhandari, G. Faulkner, E. Xie, J. J. D. McKendry, E. Gu, M. D. Dawson and D. O’Brien, “Optimum Device and Modulation Scheme Selection for Optical Wireless Communications,” *Journal of Lightwave Technology,* vol. 39, no. 8, pp. 2281 - 2287, 2021.

[43] . J. M. Smith, . R. Ley, M. S. Wong, Y. H. Baek, . J. . H. Kang, C. H. Kim, M. J. Gordon, S. Nakamura, J. S. Speck and S. P. DenBaars, “Comparison of size-dependent characteristics of blue and green InGaN microLEDs down to 1 μm in diameter,” *Applied Physics Letters,* vol. 116, no. 7, 2020.

[44] P. Deng and M. Kavehrad, *Effect of white LED DC-bias on modulation speed for visible light communications,* arXiv preprint arXiv:1612.08477, 2016.

[45] A. Alexeev, J.-P. M. Linnartz, G. Onushkin, K. Arulandu and G. Martin, “Dynamic response-based LEDs health and temperature monitoring,” *Measurement,* vol. 156, p. 107599, 2020.

[46] X. Deng, Y. Wu, A. M. Khalid, X. Long and J.-P. M. G. Linnartz, “LED power consumption in joint illumination and communication system,” *Optics Express,* vol. 25, no. 16, pp. 18990-19003, 2017.

[47] S. Mardani and J.-P. Linnartz, “Capacity of the first-order low-pass channel with power constraint,” in *2018 Symposium on Information Theory and Signal Processing in hte Benelux*, Enschede, 2018.

[48] J.-P. Linnartz, Wireless Communication: The Interactive Multimedia CD-ROM, London: Springer, 2001.

[49] J. G. Smith, “The information capacity of amplitude- and variance-constrained sclar gaussian channels,” *Information and Control,* vol. 18, no. 3, pp. 203-219, 1971.

[50] H. Qian, S. J. Yao, S. Z. Cai and T. Zhou, “Adaptive Postdistortion for Nonlinear LEDs in Visible Light Communications,” *IEEE Photonics Journal,* vol. 6, no. 4, 2014.

[51] M. Schetzen, “Nonlinear system modeling based on the Wiener theory,” *Proceedings of the IEEE,* vol. 69, no. 12, pp. 1557 - 1573, 1981.

This project has received funding from the European Union’s Horizon 2020 research and innovation programme under grant agreement No 825651 (ELIOT)

[52] D. Tsonev, S. Sinanovic and H. Haas, "Complete Modeling of Nonlinear Distortion in OFDM-Based Optical Wireless Communication," *Journal of Lightwave Technology,* vol. 31, no. 18, pp. 3064 - 3076, 2013.

[53] H. Elgala, R. Mesleh and H. Haas, "Indoor optical wireless communication: potential and state-of-the-art," *IEEE Communications Magazine,* vol. 49, no. 9, pp. 56 - 62, 2011.

[54] K. Ying, Z. Yu, R. J. Baxley, H. Qian, G.-K. Chang and G. T. Zhou, "Nonlinear distortion mitigation in visible light communications," *IEEE Wireless Communications,* vol. 22, no. 2, pp. 36 - 45, 2015.

[55] I. Neokosmidis, T. Kamalakis, J. W. Walewski, B. Inan and T. Sphicopoulos, "Impact of Nonlinear LED Transfer Function on Discrete Multitone Modulation: Analytical Approach," *Journal of Lightwave Technology,* vol. 27, no. 22, pp. 4970 - 4978, 2009.

[56] H. Elgala, R. Mesleh and H. Haas, "Predistortion in Optical Wireless Transmission Using OFDM," in *Ninth International Conference on Hybrid Intelligent Systems*, Shenyang, China, 2009.

[57] G. Stepniak, J. Siuzdak and P. Zwierko, "Compensation of a VLC Phosphorescent White LED Nonlinearity by Means of Volterra DFE," *IEEE Photonics Technology Letters,* vol. 25, no. 16, pp. 1597 - 1600, 2013.

[58] T. Kamalakis, J. W. Walewski, G. Ntogari and G. Mileounis, "Empirical Volterra-Series Modeling of Commercial Light-Emitting Diodes," *Journal of Lightwave Technology,* vol. 29, no. 14, pp. 2146 - 2155, 2011.

[59] X. Deng, S. Mardanikorani, K. Arulandu and J.-P. M. G. Linnartz, "Novel Post-Distortion to Mitigate LED Nonlinearity in High-Speed Visible Light Communications," in *IEEE Globecom Workshops (GC Wkshps)*, Abu Dhabi, United Arab Emirates, 2018.

[60] A. Alexeev, Characterization of light emitting diodes with transient measurements and simulations, Eindhoven: Technische Universiteit Eindhoven, 2020.

[61] H. Haas and T. Fath, "Performance Comparison of MIMO Techniques for Optical Wireless Communications in Indoor Environments," *IEEE Transactions on Communications,* vol. 61, no. 2, pp. 733-742, February 2013.

[62] K. L. Bober, S. M. Mana, M. Hinrichs, S. M. Kouhini, C. Kottke, D. Schulz, C. Schmidt, R. Freund and V. Jungnickel, "Distributed Multiuser MIMO for LiFi in Industrial Wireless Applications," *Journal of Lightwave Technology,* vol. 39, no. 11, pp. 3420-3433, 2021.

[63] T. E. B. Cunha, J. -P. M. G. Linnartz and X. Deng, "Achievable rate of LED-based distributed MIMO OWC systems under a per-LED power constraint," in *17th International Symposium on Wireless Communication Systems (ISWCS)*, 2021.

[64] "Modulation Techniques for Li-Fi," *ZTE COMMUNICATIONS,* vol. 14, pp. 29-40, 2016.

[65] S. D. Dissanayake and J. Armstrong, "Comparison of ACO-OFDM, DCO-OFDM and ADO-OFDM in IM/DD Systems," *Journal of Lightwave Technology,* vol. 31, no. 7, pp. 1063 - 1072, 2013.

[66] X. Li, J. Vucic, V. Jungnickel and J. Armstrong, "On the Capacity of Intensity-Modulated Direct-Detection Systems and the Information Rate of ACO-OFDM for Indoor Optical Wireless Applications," *IEEE Transactions on Communications,* vol. 60, no. 3, pp. 799 - 809, 2012.

[67] X. Li, R. Mardling and J. Armstrong, "Channel Capacity of IM/DD Optical Communication Systems and of ACO-OFDM," in *IEEE International Conference on Communications*, Glasgow, UK, 2007.

[68] J. Armstrong and B. J. Schmidt, "Comparison of asymmetrically clipped optical OFDM and DC-biased optical OFDM in AWGN," *IEEE Communications Letters,* vol. 12, no. 5, pp. 343-345, 2008.

[69] N. Fernando, Y. Hong and E. Viterbo, "Flip-OFDM for Unipolar Communication Systems," *IEEE Transactions on Communications,* vol. 60, no. 12, pp. 3726 - 3733, 2012.

[70] S. Mardani, X. Deng and J. Linnartz, "Efficiency of Power Loading Strategies for Visible Light Communication," in *2018 IEEE Globecom Workshops (GC Wkshps)*, 2018.

[71] Y. Zhai, H. Chi, J. Tong and J. Xi, "Capacity Maximized Linear Precoder Design for Spatial-Multiplexing MIMO VLC Systems," *IEEE Access,* vol. 8, pp. 63901-63909, 2020.

[72] S. M. Kouhini, S. M. Mana, R. Freund, V. Jungnickel, C. R. B. Corrêa, E. Tangdiongga, X. Deng and J.-P. M. G. Linnartz, "Distributed MIMO Experiment Using LiFi Over Plastic Optical Fiber," in *2020 IEEE Globecom Workshops (GC Wkshps)*, 2020.

[73] H. Shen, Y. Wu, W. Xu and C. Zhao, "Optimal Power Allocation for Downlink two-User Non-Orthogonal Multiple Access in Visible Light Communication," *Journal of Communications and Information Networks,* vol. 2, no. 4, pp. 57-64, Dec. 2017.

[74] L. An, H. Shen, J. Wang, Y. Zeng and R. Ran, "Energy Efficiency Optimization for MIMO Visible Light Communication Systems," *IEEE Wireless Communications Letters,* vol. 9, no. 4, pp. 452-456, 2020.

[75] J. Panta, P. Saengudomlert, K. L. Sterckx and A. T. Pham, "Performance optimisation of indoor SVD-based MIMO-OFDM optical wireless communication systems," *IET Optoelectronics,* vol. a4, no. 4, pp. 159-168, 2020.

[76] M. Grant and S. Boyd, "CVX: Matlab software for disciplined convex programming, version 2.1," Mar. 2021. [Online]. Available: http://cvxr.com/cvx.

[77] Lumiled, "Advance Electrical Design LED model, Technique notes AB20-3A," 2002.

This project has received funding from the European Union's Horizon 2020 research and innovation programme under grant agreement No 825651 (ELIOT)

[78] P. W. Berenguer, D. Schulz , J. Hilt, P. Hellwig, G. Kleinpeter, J. K. Fischer and V. Jungnickel , “Optical Wireless MIMO Experiments in an Industrial Environment,” *IEEE Journal on Selected Areas in Communications,* vol. 36, no. 1, pp. 185 - 193, 2017.

[79] P. W. Berenguer, V. Jungnickel and J. K. Fischer, “The benefit of frequency-selective rate adaptation for optical wireless communications,” in *10th International Symposium on Communication Systems, Networks and Digital Signal Processing (CSNDSP)*, Prague, Czech Republic, 2016.

[80] F. Deng, X. Yue , X. Fan, S. Guan, Y. Xu and J. Chen, “Multisource Energy Harvesting System for a Wireless Sensor Network Node in the Field Environment,” *IEEE Internet of Things Journal,* vol. 6, no. 1, pp. 918 - 927, 2019.

[81] T. Fath and H. Haas , “Performance Comparison of MIMO Techniques for Optical Wireless Communications in Indoor Environments,” *IEEE Transactions on Communications,* vol. 61, no. 2, pp. 733 - 742, 2012.

[82] Y. M. Hwang, J. H. Park, Y. Shin, J. Y. Kim and D. I. Kim , “Transmission Power and Antenna Allocation for Energy-Efficient RF Energy Harvesting Networks with Massive MIMO,” *Energies,* vol. 10, no. 6, p. 802, 2017.

[83] J. Kahn and J. Barry, “Wireless infrared communications,” *Proceedings of the IEEE,* vol. 85, no. 2, pp. 265-298, 1997.

[84] S. Karpov, “ABC-model for interpretation of internal quantum efficiency and its droop in III-nitride LEDs: a review,” *Optical and Quantum Electronics,* vol. 47, no. 6, p. 1293–1303, 2015.

[85] T. McDonald, E. Persson, A. Bricconi and F. Grawert, “GaN in a Silicon world: competition or coexistence?,” in *IEEE Applied Power Electronics Conference and Exposition (APEC)*, Long Beach, CA, 2016.

[86] M. Poenot, A. Tsiatmas and J. M. Linnartz, “Wireless infrared propagation in dense cellular sensor networks,” in *ICT Open*, Eindhoven, The Netherlands, 2013.

[87] C. Shannon, “Communication in the Presence of Noise,” *Proceedings of the IRE ,* vol. 37, no. 1, pp. 10 - 21, 1949.

[88] U. Tifize and C. Schenk, Halbleiter Schaltungstechnik, Berlin : Springer, 1986.

[89] R. Windisch, A. Knobloch, M. Kuijk, C. Rooman, B. Dutta, P. Kiesel, G. Borghs, G. H. Dohler and P. Heremans, “Large-signal-modulation of high-efficiency light-emitting diodes for optical communication,” *IEEE Journal of Quantum Electronics,* vol. 36, no. 12, pp. 1445 - 1453, 2000.

This project has received funding from the European Union’s Horizon 2020 research and innovation programme under grant agreement No 825651 (ELIOT)

[90] H. Yang, J. W. M. Bergmans, T. C. W. Schenk, J.-P. M. G. Linnartz and R. Rietman, "An analytical model for the illuminance distribution of a power LED," *Optics Express,* vol. 16, no. 26, pp. 21641-21646, 2008.

[91] J. Zhu and S. Papavassiliou, "On the energy-efficient organization and the lifetime of multi-hop sensor networks," *IEEE Communications Letters ,* vol. 7, no. 11, pp. 537 - 539, 2003.

[92] Ericsson , "Internet of Things Forecast," 2019.

[93] I. Qualcomm Technologies, "Snapdragon X24 LTE modem," 2018. [Online]. Available: https://www.qualcomm.com/products/snapdragonx24-lte-modem .

[94] I. Qualcomm Technologies, "Snapdragon X50 5G modem," 2018. [Online]. Available: https://www.qualcomm.com/media/documents/files/qualcommsnapdragon-x50-5g-modem-infographic.pdf.

[95] Hinrichs, M. et al., "A Physical Layer for Low Power Optical Wireless Communications," *IEEE Transactions on Green Communications and Networking,* vol. 5, pp. 4-17, March 2021.

[96] R. Winston, J. C. Miñano and P. Benítez, Nonimaging Optics, Elsevier Academic Press, 2005.

[97] A. Riaz and S. Collins, "A wide field of view VLC receiver for smartphones," in *2020 European Conference on Optical Communications (ECOC)*, 2020.

[98] X. Deng, S. Mardanikorani, G. Zhou and J. -P. M. G. Linnartz, "DC-Bias for Optical OFDM in Visible Light Communications," *IEEE Access,* vol. 7, pp. 98319-98330, 2019.

This project has received funding from the European Union's Horizon 2020 research and innovation programme under grant agreement No 825651 (ELIOT)